Journal of Food Protection, Vol. 85, No. 9, 2022, Pages 1335–1354
https://doi.org/10.4315/JFP-22-025

Research Paper

Development of a Modeling Tool To Assess and Reduce Regulatory and Recall Risks for Cold-Smoked Salmon Due to *Listeria monocytogenes* Contamination

RUIXI CHEN *https://orcid.org/0000-0002-3663-9768*, **RENATO H. ORSI** *https://orcid.org/0000-0003-4933-9817*, **VERONICA GUARIGLIA-OROPEZA** *https://orcid.org/0000-0001-7851-2514*, **AND MARTIN WIEDMANN** *https://orcid.org/0000-0002-4168-5662**

Department of Food Science, Cornell University, Ithaca, New York 14853, USA

MS 22-025: Received 27 January 2022/Accepted 14 June 2022/Published Online 20 June 2022

ABSTRACT

Although public health risk assessments for *Listeria monocytogenes* (*Lm*) have been published for various foods, firm-level decision making on interventions targeting *Lm* involves considerations of both public health and enterprise risks. Smoked seafood is a ready-to-eat product with a high incidence of *Lm* contamination and has been associated with several recalls. We used cold-smoked salmon as a model product to develop a decision support tool (the regulatory and recall risk [3R] model) to estimate (i) baseline regulatory and recall (RR) risks (i.e., overall risks of a lot sampled and found positive for *Lm,* e.g., by food regulatory agencies) due to *Lm* contamination and (ii) the RR risk reduction that can be achieved through interventions with underlying mechanisms such as reducing the prevalence and/or level of *Lm* and retarding or preventing *Lm* growth. Given that a set number of samples (e.g., 10) are tested for a given lot, the RR risk equals the likelihood of detecting *Lm* in at least one sample. Under the baseline scenario, which assumes a 4% *Lm* prevalence and no interventions, the median predicted RR risk for a given production lot was 0.333 (95% credible interval: 0.288, 0.384) when 10 25-g samples were tested. Nisin treatments, which reduce both the prevalence and initial level of *Lm,* reduced RR risks in a concentration-dependent manner to 0.109 (0.074, 0.146) with 5 ppm, 0.049 (0.024, 0.083) with 10 ppm, and 0.017 (0.007, 0.033) with 20 ppm. In general, more effective reduction in RR risks can be achieved by reducing *Lm* prevalence than by retarding *Lm* growth; the RR risk was reduced to 0.182 (0.153, 0.213) by a 50% prevalence reduction but to only 0.313 (0.268, 0.367) by bacteriostatic growth inhibitors. Sensitivity analysis indicated that prevalence and initial level of *Lm* and storage temperature have the greatest impact on predicting RR risks, suggesting that reliable data for these parameters will improve model performance.

HIGHLIGHTS

- A modeling framework for assessing regulatory and recall risks was developed.
- Reducing *Lm* prevalence drastically reduces regulatory and recall risks.
- Retarding growth of *Lm* has a marginal effect on regulatory and recall risks.
- Nisin treatments are most effective in reducing regulatory and recall risks.

Key words: Cold-smoked salmon; Decision support tool; *Listeria monocytogenes*; Nisin; Regulatory and recall risk

Listeria monocytogenes (*Lm*) is a foodborne pathogen that causes listeriosis, a potentially life-threatening disease that leads to 260 deaths annually in the United States *(11)*. The rate of listeriosis has been constant over the last decade, and the invasive form of the disease is most likely to occur in sensitive populations, including pregnant women (who can pass it on to their newborns) and elderly and immunocompromised individuals *(11, 32, 39)*. *Lm* is responsible for 19% of deaths due to consumption of contaminated food in the United States *(72)*. Ready-to-eat (RTE) foods that are usually consumed without further listericidal steps beyond packaging have been (i) considered of particular significance for sporadic foodborne listeriosis and (ii) associated with a number of outbreaks *(25, 29, 61)*. As a type of RTE food, smoked seafood (including cold-smoked salmon) has been classified in the high-risk category for listeriosis (more than five cases per billion servings) because these products (i) have been reported to be contaminated with *Lm* at high incidence and (ii) are able to support the growth of *Lm* to high levels during extended storage at refrigeration temperature *(37, 82)*. The prevalence of *Lm* among smoked seafood products reported since the 1990s differs across product types, countries, and years and ranges from 0 to 80.3% *(38)*. *Lm* contamination of RTE seafood products has been responsible for product recalls in

* Author for correspondence. Tel: 607-254-2838; Fax: 607-254-4868; E-mail: mw16@cornell.edu.

various countries (e.g., United States and the European Union [EU]–European economic area [EEA]). For example, 3.7 and 11.5% of the foodborne outbreaks (1998 to 2017) and food product recalls (2017 to 2020), respectively, in the United States were reported to be caused by *Lm* contamination of seafood-associated products *(12, 80)*. In the EU-EEA, 42% of seafood-related notifications reported by the Rapid Alert System for Food and Feed between 2008 and 2016 were related to *Lm,* and 19% of seafood-associated foodborne diseases outbreaks between 2008 and 2015 were caused by *Lm (71)*.

Elimination of *Lm* in smoked and RTE seafoods is challenging (and essentially not feasible) because *Lm* is widely distributed in a variety of settings, including natural and urban environments *(58),* food processing facilities *(26, 78),* and consumer homes *(22)*. However, continuous improvement of the safety of smoked seafood products with respect to *Lm* contamination is possible and needed and typically involves a variety of control strategies, targeting (i) the reduction of *Lm* prevalence and contamination levels among food products, (ii) the prevention or reduction of *Lm* growth on contaminated food products, and (iii) science-based education for at-risk populations and associated caregivers *(37)*. Interventions for reducing the prevalence of *Lm* may include raw material controls, the implementation of environmental monitoring programs, and stringently following good manufacturing practices and sanitation standard operation procedures *(37)*. Postlethality treatments such as irradiation *(87)* and high pressure processing *(54)* and product reformulation involving bacteriocins *(40, 59, 75, 76),* bacteriophages *(33, 35),* organic acids *(40, 62, 63),* or competitive lactic acid bacteria *(23, 60)* can also retard or prevent growth or even reduce the level of *Lm* on contaminated food products. Examples of more commonly used postlethality treatments for cold-smoked seafood in the United States include applications of lactate or diacetate and nisin, a U.S. Food and Drug Administration (FDA)–approved bacteriocin that is active against *Lm (72)*.

Quantitative risk assessments play an important role in informing risk management associated with *Lm* in smoked seafoods by linking food safety research findings to industry practices to eventually improve public health *(2)*. By assessing the impact of variation in parameters due to inherent heterogeneity or uncertainty regarding model outcomes, guidance can be provided to improve industry practices and select appropriate interventions for controlling *Lm*. Various *Lm* quantitative risk assessments have been conducted for RTE foods in general *(82)* and specifically for cold-smoked salmon *(20, 65, 66)*. Most of these risk assessment models were designed to provide guidance for controlling *Lm* contamination of food products and were based on public health measures (e.g., the average number of human listeriosis cases caused by one serving) as outcomes, and many of these models have suggested that practices that retard or prevent the growth of *Lm* are most effective for reducing the risk of human listeriosis. These models typically include a dose-response function, which provides a quantitative relationship between the level of *Lm* exposure and the likelihood of human listeriosis. However, the dose-response compartment of such models typically has a high level of uncertainty, and precise dose-response relationships may be difficult to derive for a variety of reasons. For example, limited or no human dose-response data are available for many pathogens, and these dose-response curves have to heavily rely on animal data. Development of biologically plausible dose-response models requires knowledge of the infection pathways, which may differ across subpopulations (e.g., pregnant women and their newborns versus other individuals) and pose a challenge for estimating public health outcomes associated with many foodborne pathogens, including *Lm (6)*.

Production company decision making on interventions targeting *Lm* typically involves both public health and enterprise risk considerations. Different regulatory consequences stem from a sampled production lot that tests positive for *Lm*. In the United States, an *Lm*-positive test on a product lot that is still under full control of the processor would likely trigger a stock recovery, whereas an *Lm*-positive test on a production lot that has been fully or partially released into commerce would typically lead to a product recall. We thus defined the term regulatory and recall (RR) risk as the overall risk of a production lot being sampled and tested positive for *Lm* (e.g., by regulatory agencies), regardless of the possible regulatory consequences. To facilitate improved decision making regarding *Listeria* control strategies, we developed a modeling framework that allows for assessment of RR risks and the impact of various interventions on reducing these risks. We developed the RR risk (3R) model to estimate the RR risks associated with presliced, vacuum-packed cold-smoked salmon products and to identify and/or optimize interventions to lower this risk. Cold-smoked salmon was selected as a model product because (i) it has been frequently associated with *Lm* contamination *(46),* (ii) it supports the growth of *Lm (19, 36),* and (iii) *Lm* contamination of cold-smoked salmon has been used as a case study in previous quantitative risk assessments *(43, 66)*. Nisin was selected as a model antimicrobial to assess the impact of antimicrobial treatments on RR risks because this bacteriocin is commonly used in food and its efficacy against *Lm* on cold-smoked salmon has been extensively studied; hence, substantial data for model development were available *(13, 40, 76)*. This 3R model will allow industry to use information on both public health and enterprise risk implications of various interventions when driving continuous improvement with regard to *Lm* control in RTE foods. The 3R model introduced here may have reduced uncertainty as compared with public health models, which may further facilitate science-based decision making.

MATERIALS AND METHODS

Model overview. The 3R model is a probabilistic decision-support tool developed to estimate the risk of recalls or other regulatory consequences due to food product contamination with *Lm*. The 3R model was developed with the R Statistical Programming Environment (R Core Team, Vienna, Austria) v. 3.5.2 *(70)*; data and R codes used are available on GitHub (https://github.com/FSL-MQIP/RegulatoryAndRecallRiskModel_

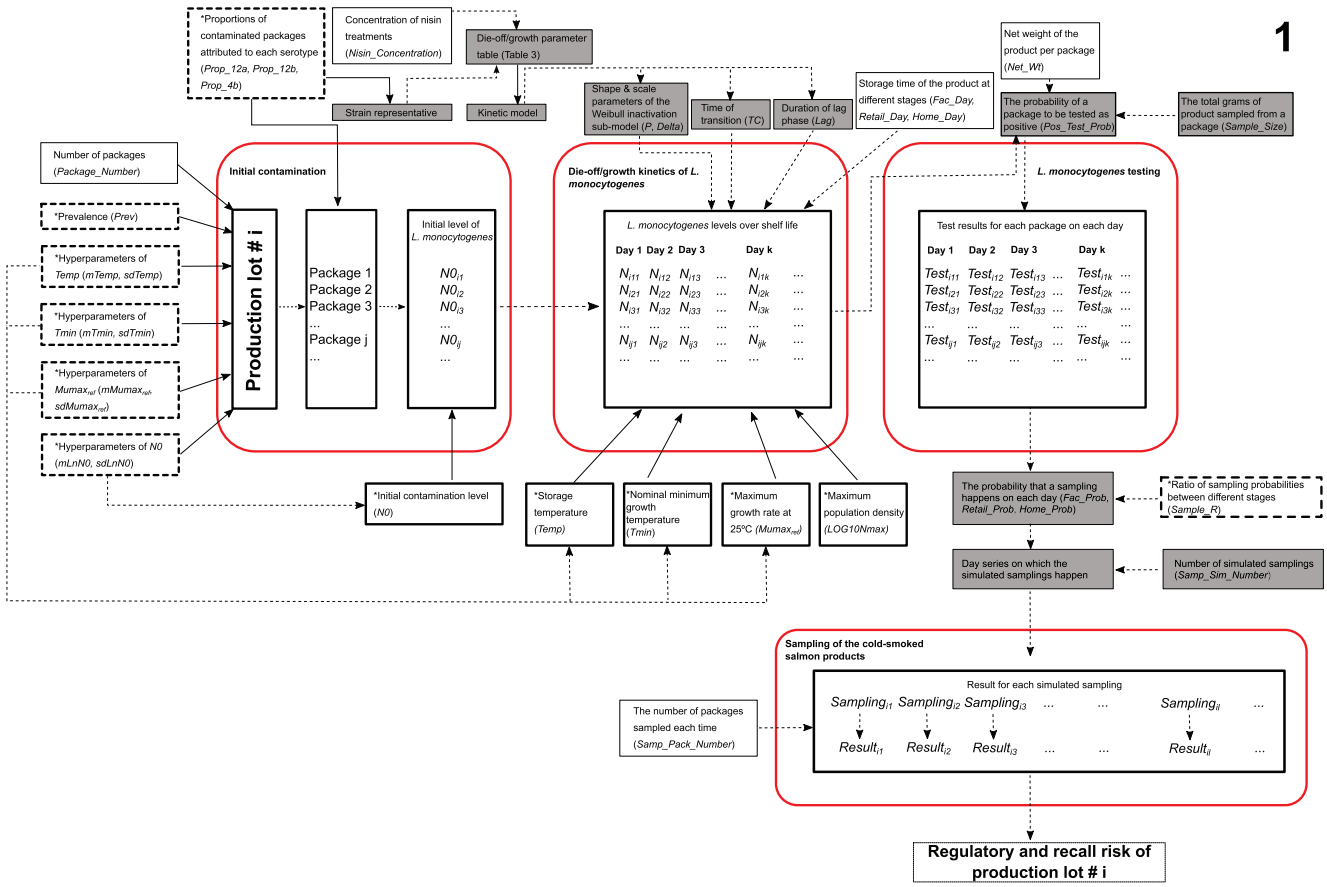

FIGURE 1. *Schematic of the 3R model. Only a single production lot (lot* i*) is shown for clarity of demonstration of the subprocesses. The same schematic is applicable to all production lots. Red rectangles delineate distinct subprocesses. Bold rectangles delineate variable parameters. Bold dashed rectangles delineate uncertain parameters. Shaded rectangles delineate parameters for which the values are either fixed or determined conditional on the values of other parameters. Rectangles without shading delineate user inputs. Solid arrows indicate stochastic dependences, and dashed arrows indicate logic links. All model parameters are described in detail in Table 1.* N_{ijk} *denotes the number of* Lm *cells in the* j*th package of the* i*th production lot on the* k*th day after the end of processing.* $Test_{ijk}$ *denotes the binary (presence or absence) result of* Lm *testing for the* j*th package of the* i*th production lot on the* k*th day after the end of processing.* $Sampling_{il}$ *denotes the* l*th simulated sampling of the* i*th production lot, which has a binary result (whether at least one package was sampled and tested positive for* Lm*) designated as* $result_{il}$.

Listeria_ColdSmokedSalmon.git). The model encompasses the whole shelf life of vacuum-packed, RTE cold-smoked salmon, including storage at the processing facility, retail stores, and consumer homes. The model includes four subprocesses: (i) initial *Lm* contamination of cold-smoked salmon products at the end of processing (i.e., zero days of storage), (ii) die-off and growth kinetics of *Lm* on contaminated products throughout the shelf life, (iii) sampling of products (e.g., by food regulatory agencies) at the facility, retail stores, and/or consumer homes (under rare but possible circumstances, such as in cases of consumer complaints or outbreak investigations), and (iv) detection of *Lm* on the collected samples, which is an essential part of the model because it determines whether regulatory consequences (e.g., recalls) should be initiated.

In the model simulation, 1,000 production lots of cold-smoked salmon products are generated, each containing 10,000 packages. The storage temperature of a single package is assumed to be constant over the shelf life (see Table 1 for details on all model parameters). The model outcome is the RR risk of a production lot of cold-smoked salmon product produced under a given scenario. Details on the modeling process (see Fig. 1) are described specifically in the following sections.

Simulation framework. In our 3R model, variability refers to the irreducible, inherent variation of the studied system, whereas uncertainty arises from the lack of knowledge, which can be reduced by acquisition of additional information *(56)*. Although both uncertainty and variability contribute variation to model outcomes, interpretation with respect to the uncertain and variable components of the model may provide different insights for guiding industry practices; key sources of variability are typically useful for identifying interventions, and key sources of uncertainty are typically useful for prioritizing additional data collection and/or research. Therefore, we modeled variability and uncertainty separately, as also detailed by National Research Council *(55)* and Codex Alimentarius Commission *(15)* documents on risk assessments, by using a second-order Monte Carlo simulation framework, consistent with a number of previous risk assessments *(20, 64, 66, 83, 85)*. We assumed that variability exists across different packages within a given lot (e.g., because different packages may be exposed to different temperatures during distribution) and that uncertainty exists across different lots (e.g., typically due to insufficient data on the actual initial contamination prevalence for each lot). This dissection of variability and uncertainty was mainly based on considerations

TABLE 1. *Detailed information of the model parameters*

Notation	Description	Parameter status	Value, distribution	Baseline	Unit	Reference(s)
Product parameters						
Lot_Number	No. of simulated production lots	Fixed	1,000	1,000	Lot	Current model
Package_Number	No. of simulated packages per lot	Fixed	10,000	10,000	Package	Current model
Fac_Day	No. of storage days at the facility	Fixed	User defined	10	Day	Expert opinion
Retail_Day	No. of storage days at retail stores	Fixed	User defined	30	Day	Expert opinion
Home_Day	No. of storage days at consumer homes	Fixed	User defined	20	Day	Expert opinion
Net_Wt	Net weight of the product per package	Fixed	User defined	100	Gram	Expert opinion
Nisin_Concentration	Concn of the nisin treatments	Fixed	Discrete values: 0, 5, 10, 20; user defined	0	ppm	Current model
Subprocess: initial contamination						
Prev	Prevalence of *Lm*	Uncertain	$Beta(\text{shape1} = 118.50, \text{shape2} = 2831.50)$	0.04	No unit	*38, 52*
N0	Initial contamination level of *Lm*	Variable	$\ln(N0) \sim Truncated\ Normal[\text{mean} = mLnN0, \text{sd} = sdLnN0, a = \ln(\frac{1}{Net\_Wt}), b = +\infty]^{a,b}$	*Truncated Normal* (mean = −1.78, sd = 1.07, $a = -4.61, b = +\infty$)	CFU/g	*5*
mLnN0	Mean of the ln(*N0*) distribution	Uncertain	$Normal(\text{mean} = -1.78, \text{sd} = 0.13)$	−1.78	Ln CFU/g	Current model
sdLnN0	SD[c] of the ln(*N0*) distribution	Uncertain	$Normal(\text{mean} = 1.07, \text{sd} = 0.16)$	1.07	Ln CFU/g	Current model
Subprocess: die-off, growth kinetics of *Lm* on contaminated cold-smoked salmon products						
Temp	Storage temp	Variable	$Normal(\text{mean} = mTemp, \text{sd} = sdTemp)$	*Normal*(mean = 4.4, sd = 0.77)	°C	*1*
mTemp	Mean of the *Temp* distribution	Uncertain	$Normal(\text{mean} = 4.4, \text{sd} = 1.9)$	4.4	°C	*1*
sdTemp	SD of the *Temp* distribution	Uncertain	$Gamma(\text{shape} = 0.7, \text{scale} = 1.1)$	0.77	°C	*1*
$Mumax_{ref}$	Maximum growth rate of *Lm* at the reference temp (25°C)	Variable	$Truncated\ Normal(\text{mean} = mMumax_{ref}, \text{sd} = sdMumax_{ref}, a = 0, b = +\infty)^{b}$	*Truncated Normal* (mean = 6.71, sd = 2.54, $a = 0, b = +\infty$)	Day^{-1}	*20*
$mMumax_{ref}$	Mean of the $Mumax_{ref}$ distribution	Uncertain	$Normal(\text{mean} = 6.71, \text{sd} = 0.26)$	6.71	Day^{-1}	*14, 20, 40, 76*
$sdMumax_{ref}$	SD of the $Mumax_{ref}$ distribution	Uncertain	$\ln(sdMumax_{ref}) \sim Gamma(\text{shape} = 159.88, \text{scale} = 0.006)$	0.36	Day^{-1}	*14, 20, 40, 76*
Mumax	Maximum growth rate of *Lm* at the actual temp	Dependent	$0 (Temp \leq Tmin)$ $Mumax_{ref} \cdot \left(\frac{Temp - Tmin}{25 - Tmin}\right)^2 (Temp > Tmin)$	NA	Day^{-1}	Current model
Tmin	Nominal minimum growth temp of *Lm*	Variable	$Normal(\text{mean} = mTmin, \text{sd} = sdTmin)$	*Normal*(mean = −2.86, sd = 1.89)	°C	*20*
mTmin	Mean of the *Tmin* distribution	Uncertain	$Normal(\text{mean} = -2.86, \text{sd} = 0.46)$	−2.86	°C	*20*
sdTmin	SD of the *Tmin* distribution	Uncertain	$\ln(sdTmin) \sim Normal(\text{mean} = 0.64, \text{sd} = 0.21)$	1.89	°C	*20*
LOG10Nmax	Maximum population density of *Lm*	Variable	$Weibull(\text{shape} = 41.34, \text{scale} = 9.13)$ $(nisin\_concentration = 0\ \text{ppm})$ $Weibull(\text{shape} = 21.60, \text{scale} = 8.71)$ $(nisin\_concentration = 5\ \text{ppm})$ $Weibull(\text{shape} = 14.55, \text{scale} = 8.50)$ $(nisin\_concentration = 10\ \text{ppm})$ $Weibull(\text{shape} = 8.44, \text{scale} = 8.21)$ $(nisin\_concentration = 20\ \text{ppm})$	*Weibull*(shape = 41.34, scale = 9.13)	Log CFU/g	*13, 14, 40, 76*

TABLE 1. *Continued*

Notation	Description	Parameter status	Value, distribution	Baseline	Unit	Reference(s)
Prop_12a	Proportion of the contaminated packages attributed to serotype 1/2a	Uncertain	$Dirichlet(\alpha)$ $\alpha = (1,1,1)$	0.33	No unit	Expert opinion
Prop_12b	Proportion of the contaminated packages attributed to serotype 1/2b	Uncertain		0.33	No unit	
Prop_4b	Proportion of the contaminated packages attributed to serotype 4b	Uncertain		0.33	No unit	
P	Shape parameter of the Weibull inactivation submodel	Dependent	See Table 2	NA	No unit	Current model
Delta	Scale parameter of the Weibull inactivation submodel (i.e., time for the first decimal reduction of population density)	Dependent	See Table 2	NA	Day	Current model
TC	Time when *Lm* transits from the die-off to the regrowth phase	Dependent	See Table 2	NA	Day	Current model
Lag	Duration of the lag phase	Dependent	See Table 2	NA	Day	Current model
Subprocess: *Lm* testing						
Sample_Size	Total grams sampled from a single package	Fixed	25	25	Gram	*81*
Pos_Test_Prob	Probability that a contaminated package tests positive for *Lm* (given *N* bacterial cells within)	Dependent	$\frac{(Net_{Wt}-N)!/(Net_{Wt}-Sample_{Size})!}{(Net_{Wt}-Sample_{Size})!/Sample_{Size}!}\cdot 100$ $(0<N<22)$ $99.9(N\geq 22)$	NA	%	Expert opinion
Subprocess: sampling of cold-smoked salmon products						
Sampling_R	Ratio of the sampling likelihood between facility stage and retail store stage, and between retail store stage and consumer home stage	Uncertain	$Uniform(\min = 1, \max = 10)$	5	No unit	Expert opinion
Fac_Prob	Probability that a sampling happens on a given day at the facility	Dependent	$\frac{Sampling\_R^2}{(Fac\_Day\cdot Sampling\_R^2+Retail\_Day\cdot Sample\_R+Home\_Day)}$	5.95	%	Expert opinion
Retail_Prob	Probability that a sampling happens on a given day at retail stores	Dependent	$\frac{Fac\_Prob}{Sampling\_R}$	1.19	%	Expert opinion
Home_Prob	Probability that a sampling happens on a given day at consumer homes	Dependent	$\frac{Fac\_Prob}{Sampling\_R^2}$	0.24	%	Expert opinion
Samp_Sim_Number	No. of simulated samplings for a given production lot	Fixed	10,000	10,000	Sampling	Current model
Samp_Pack_Number	No. of products sampled per sampling	Fixed	User defined	10	Package	Expert opinion

[a] Where ln is the natural logarithm.
[b] Where *a* and *b* refer to the lower and upper bounds of truncated distributions, respectively.
[c] SD, standard deviation.

on the sufficiency of existing data for modeling various factors. Consequently, for the variables of storage temperature, initial contamination level, maximum growth rate at the reference temperature (25°C), and nominal minimum growth temperature, the variability component was modeled by characterizing the variation across different packages based on a parametric distribution, and the uncertainty component was modeled by allowing the hyperparameters of this distribution to vary across different lots in their own parameter space. The contribution of other product characteristics (e.g., pH, water phase salt content, and phenolic compound concentration) to the model outcome was accounted for through the variability and uncertainty of the maximum growth rate at the reference temperature *(20)*. Lot-level factors, including prevalence of *Lm* contamination and proportion of contaminated products with each of the three *Lm* serotypes commonly associated with cold-smoked salmon production (serotypes 1/2a, 1/2b, and 4b), were allowed to vary only across lots; the variation of these factors was generally considered uncertain because their associated distribution was inferred from limited data. The variability of maximum population density of *Lm* across packages within a given lot was modeled with no uncertainty because (i) substantial data were available for inferring the variability distribution and (ii) this factor was assumed less important for predicting RR risks because in most cases any samples with *Lm* levels at the maximum population density, regardless of its actual value, will have the same likelihood of yielding a positive test. The dissection of the variability and uncertainty components of the model resulted in classification of the model parameters into variable and uncertain parameters, which are detailed in Table 1 and further described in sections below.

Variable parameters and distributions. The parametric distributions (Table 1) for storage temperature (*Temp*), nominal minimum growth temperature (*Tmin*), and maximum growth rate at the reference temperature ($Mumax_{ref}$) were based on previous studies *(1, 20)*. Censored data *(5)* for initial *Lm* contamination level (*N0*) were fitted with a variety of parametric distributions using a maximum likelihood estimation in the fitdistrplus v. 1.0.14 package *(21)*. Distributions were compared by visualizing the goodness-of-fit graphs; the distribution that best approximated the empirical distribution of the data was selected as the best-fit model. For maximum population density (*LOG10Nmax*), data obtained from previous studies *(13, 76)* were fitted with various parametric distributions, which were compared using the Anderson-Darling statistic *(73)*.

Uncertain parameters and distributions. The distribution for *Lm* prevalence in a given lot (*Prev*) was inferred following the Bayesian approach described by Miconnet et al. *(52)*. Beta (0.5, 0.5) was specified as the prior distribution for *Prev,* which was iteratively updated using the data obtained from three studies that reported the prevalence of *Lm* in smoked seafood products in the United States *(31, 42, 77)*. The posterior distribution estimated at the last iteration was used to characterize the uncertainty of *Prev.* The proportions of contaminated packages attributed to *Lm* serotypes 1/2a, 1/2b, and 4b (*Prop_12a, Prop_12b,* and *Prop_4b*) was assumed to follow a Dirichlet distribution (Table 1).

Parameters used to define the parametric distributions of variable parameters, referred to as hyperparameters, are also considered in the model as uncertain parameters. Distributions of the hyperparameters (Table 1) for *Temp* (*mTemp* and *sdTemp*) and *Tmin* (*mTmin* and *sdTmin*) were specified based on previous studies *(1, 20)*. Distributions of the hyperparameters of *N0* (*mLnN0* and *sdLnN0*) were inferred through a bootstrap resampling method using the fitdistrplus v. 1.0.14 package. Distributions of the hyperparameters of $Mumax_{ref}$ ($mMumax_{ref}$ and $sdMumax_{ref}$) were inferred following a Bayesian approach using the BayesianTools v. 0.1.7 package *(34)*. The distributions for $mMumax_{ref}$ and $sdMumax_{ref}$ reported by Delignette-Muller et al. *(20)* were used as prior distributions, which were updated using additional data for $Mumax_{ref}$ obtained from challenge studies for *Lm* on cold-smoked salmon *(40, 76)* and unpublished work by our laboratory *(14)*. Three independent Markov chain Monte Carlo (MCMC) chains (with the Metropolis algorithm), each with 10,000 iterations, were performed using various starting values for $mMumax_{ref}$ and $sdMumax_{ref}$ randomly selected from their respective prior distribution. The first 5,000 iterations of each MCMC chain were considered the adaptation phase and discarded; the 5,000 iterations following the adaptation phase of each MCMC chain were pooled to generate empirical distributions for $mMumax_{ref}$ and $sdMumax_{ref}$, respectively. Empirical distributions were then fitted with a variety of parametric distributions, and the best-fit distribution for each hyperparameter was determined based on the Anderson and Darling statistic.

Modeling the initial contamination of production lots. The prevalence and initial contamination levels of *Lm* for each production lot are characterized by a value for *Prev* and hyperparameters of *N0* (*mLnN0* and *sdLnN0*), which are considered fixed for a given lot. Based on *Prev,* a given number of packages is determined to be contaminated with *Lm* for each production lot. Based on *mLnN0* and *sdLnN0,* a lognormal distribution is specified for *N0* for each production lot; values of *N0* are randomly drawn from this distribution and assigned to each contaminated package within a given lot.

Modeling the die-off and/or growth kinetics of *Lm* on contaminated cold-smoked salmon products. To describe the die-off and growth kinetics of *Lm* levels on cold-smoked salmon treated with nisin, we constructed a set of primary models for describing both the initial die-off phase and the following regrowth phase (designated as die-off & regrowth models; Table 2) using data on die-off and growth for four *Lm* strains obtained through a challenge study of cold-smoked salmon treated with 0, 5, 10, or 20 ppm of nisin *(40)*. A nonlinear (Weibull) submodel was used to describe the microbial inactivation *(45)* caused by nisin treatments, and this submodel was mathematically linked to one of five different primary growth models (Table 2): (i) the three-phase linear model described by Buchanan et al. *(7),* (ii) the two-phase version (without lag phase) of the Buchanan model, (iii) the nonlinear model proposed by Baranyi and Roberts *(4),* (iv) the Baranyi and Roberts model without lag phase, and (v) the modification of the nonlinear Gompertz model as described by Gibson et al. *(30)* and reparameterized by Zwietering et al. *(89).* *Lm* enumeration data from the cold-smoked salmon challenge study *(40)* were fitted with either the primary growth models (for salmon without nisin treatments) or the die-off & regrowth models (for salmon treated with nisin), using a modification of the Levenberg-Marquardt algorithm implemented in the minpack.lm v. 1.2-1 package *(24)*. For each combination of *Lm* strain and nisin concentration, the goodness of fit across models was compared based on the Bayesian information criterion (BIC) model weight *(3, 9, 44)* using the AICcmodavg v. 2.2-2 package *(47)*; the model (s) with the highest BIC model weight and the associated parameter values were selected to describe the *Lm* die-off and growth kinetics (Table 3). Depending on the model, different die-off and growth parameters may be needed: (i) the shape (*P*) and

TABLE 2. *Mathematical equations of the primary growth and die-off & regrowth models*

Model	Equation[a]	Reference(s)
Primary growth models		
Buchanan	$LOG10N = LOG10N0 (0 \le t < Lag)$	*7*
	$LOG10N = LOG10N0 + Mumax \cdot t \quad \left[Lag \le t < Lag + \frac{(LOG10Nmax - LOG10N0)}{Mumax}\right]$	
	$LOG10N = LOG10Nmax \left[t \ge Lag + \frac{(LOG10Nmax - LOG10N0)}{Mumax}\right]$	
Buchanan without lag	$LOG10N = LOG10N0 + Mumax \cdot t \quad \left[0 \le t < \frac{(LOG10Nmax - LOG10N0)}{Mumax}\right]$	*7*
	$LOG10N = LOG10Nmax \left[t \ge \frac{(LOG10Nmax - LOG10N0)}{Mumax}\right]$	
Gompertz	$LOG10N = LOG10N0 + (LOG10Nmax - LOG10N0) \cdot e^{-e^{\left[\frac{Mumax \cdot e \cdot (Lag - t)}{LOG10Nmax - LOG10N0} + 1\right]}} (t \ge 0)$	*30, 89*
Baranyi	$LOG10N = LOG10Nmax + \log\left\{\frac{\left[-1 + e^{(Mumax \cdot Lag)} + e^{(Mumax \cdot t)}\right]}{e^{(Mumax \cdot t)} - 1 + e^{(Mumax \cdot Lag)} \cdot 10^{(LOG10Nmax - LOG10N0)}}\right\} (t \ge 0)$	*4*
Baranyi without lag	$LOG10N = LOG10Nmax - \log\left\{1 + \left[10^{(LOG10Nmax - LOG10N0)} - 1\right] \cdot e^{(-Mumax \cdot t)}\right\} (t \ge 0)$	*4*
Die-off & regrowth models		
Weibull-Buchanan	$LOG10N = LOG10N0 - \left(\frac{t}{Delta}\right)^P (0 \le t < TC)$	*7, 45*
	$LOG10N = LOG10N0 - \left(\frac{TC}{Delta}\right)^P (TC \le t \langle Lag; Lag \rangle TC)$	
	$LOG10N = LOG10N0 - \left(\frac{TC}{Delta}\right)^P + Mumax \cdot (t - Lag) \left(Lag \left\langle t \le Lag + \left\{\frac{LOG10Nmax - \left[LOG10N0 - \left(\frac{TC}{Delta}\right)^P\right]}{Mumax}\right\}; Lag \right\rangle TC\right)$	
	$LOG10N = LOG10Nmax \left(t > Lag + \left\{\frac{LOG10Nmax - \left[LOG10N0 - \left(\frac{TC}{Delta}\right)^P\right]}{Mumax}\right\}; Lag > TC\right)$	
Weibull-Buchanan without lag	$LOG10N = LOG10N0 - \left(\frac{t}{Delta}\right)^P (0 \le t < TC)$	*7, 45*
	$LOG10N = LOG10N0 - \left(\frac{TC}{Delta}\right)^P + Mumax \cdot (t - TC) \left(TC \le t < TC + \left\{\frac{LOG10Nmax - \left[LOG10N0 - \left(\frac{TC}{Delta}\right)^P\right]}{Mumax}\right\}\right)$	
	$LOG10N = LOG10Nmax \left(t \ge TC + \left\{\frac{LOG10Nmax - \left[LOG10N0 - \left(\frac{TC}{Delta}\right)^P\right]}{Mumax}\right\}\right)$	
Weibull-Gompertz	$LOG10N = LOG10N0 - \left(\frac{t}{Delta}\right)^P (0 \le t < TC)$	*30, 45, 89*
	$LOG10N = LOG10N0 - \left(\frac{TC}{Delta}\right)^P + \left\{LOG10Nmax - \left[LOG10N0 - \left(\frac{TC}{Delta}\right)^P\right]\right\} \cdot e^{-e^{\left\{\frac{Mumax \cdot e \cdot (Lag - TC - t)}{LOG10Nmax - \left[LOG10N0 - \left(\frac{TC}{Delta}\right)^P\right]} + 1\right\}}} (t \ge TC; Lag > TC)$	
Weibull-Baranyi	$LOG10N = LOG10N0 - \left(\frac{t}{Delta}\right)^P (0 \le t < TC)$	*4, 45*
	$LOG10N = LOG10Nmax + \log\left(\frac{-1 + e^{[Mumax \cdot (Lag - TC)]} + e^{(Mumax \cdot t)}}{e^{(Mumax \cdot t)} - 1 + e^{[Mumax \cdot (Lag - TC)]} \cdot 10^{\left\{LOG10Nmax - \left[LOG10N0 - \left(\frac{TC}{Delta}\right)^P\right]\right\}}}\right) (t \ge TC; Lag > TC)$	
Weibull-Baranyi without lag	$LOG10N = LOG10N0 - \left(\frac{t}{Delta}\right)^P (0 \le t < TC)$	*4, 45*
	$LOG10N = LOG10Nmax - \log\left(1 + 10^{\left\{LOG10Nmax - \left[LOG10N0 - \left(\frac{TC}{Delta}\right)^P\right] - 1\right\}} \cdot e^{[-Mumax \cdot (t - TC)]}\right) (t \ge TC; Lag > TC)$	

[a] *t,* time (day); *LOG10N,* population density at time *t* (log CFU/g); *LOG10N0,* initial level (log CFU/g); *Mumax,* maximum growth rate (day^{-1}); *LOG10Nmax,* maximum population density (log CFU/g); *Lag,* duration of lag phase (day); *TC,* time of transition from the die-off to the regrowth phase (day); *P,* shape parameter of the Weibull inactivation submodel (no unit); *Delta,* scale parameter of the Weibull inactivation submodel (i.e., time for the first decimal reduction in population density due to antimicrobial treatments; day).

TABLE 3. *Representative* Lm *strains and the associated primary growth and die-off & regrowth models*

Nisin, strain	Serotype	Model[a]	Weight[b]	*LOG10N0*[c]	*P*[c]	*Delta*[c]	*TC*[c]	*Lag*[c]	*Mumax*[c]	*LOG10Nmax*[c]
0 ppm										
FSL C1-0111	1/2a	Bar_nl	1	DIST	NA	NA	NA	NA	DIST	DIST
FSL F2-0237	1/2a	Bar_nl	0.50	DIST	NA	NA	NA	NA	DIST	DIST
FSL F2-0237	1/2a	Buc_nl	0.50	DIST	NA	NA	NA	NA	DIST	DIST
FSL F6-0366	4b	Bar_nl	0.51	DIST	NA	NA	NA	NA	DIST	DIST
FSL F6-0366	4b	Buc_nl	0.49	DIST	NA	NA	NA	NA	DIST	DIST
FSL L3-0051	1/2b	Buc_nl	1	DIST	NA	NA	NA	NA	DIST	DIST
5 ppm										
FSL C1-0111	1/2a	WeiBuc_nl	1	DIST	0.02	7.22E−05	8.50	NA	DIST	DIST
FSL F6-0366	4b	WeiBar_nl	1	DIST	0.65	0.48	0.64	NA	DIST	DIST
FSL L3-0051	1/2b	WeiBuc_nl	0.50	DIST	0.75	0.54	1.62	NA	DIST	DIST
FSL L3-0051	1/2b	WeiBar_nl	0.50	DIST	0.75	0.54	1.62	NA	DIST	DIST
10 ppm										
FSL C1-0111	1/2a	WeiBar_nl	1	DIST	0.51	0.41	1.58	NA	DIST	DIST
FSL F2-0237	1/2a	WeiBuc_nl	1	DIST	0.25	0.11	3.37	NA	DIST	DIST
FSL F6-0366	4b	WeiBuc_nl	1	DIST	0.11	0.11	3.39	NA	DIST	DIST
FSL L3-0051	1/2b	WeiBar	1	DIST	0.47	0.29	1.41	1.41	DIST	DIST
20 ppm										
FSL C1-0111	1/2a	WeiBar_nl	1	DIST	0.23	0.42	3.00	NA	DIST	DIST
FSL F2-0237	1/2a	WeiBar	1	DIST	0.28	0.03	0.68	8.90	DIST	DIST
FSL F6-0366	4b	WeiBuc_nl	0.51	DIST	0.28	0.38	6.34	NA	DIST	DIST
FSL F6-0366	4b	WeiBar_nl	0.49	DIST	0.28	0.38	6.38	NA	DIST	DIST
FSL L3-0051	1/2b	WeiBuc_nl	1	DIST	0.13	1.23E−03	2.76	NA	DIST	DIST

[a] The best-fit primary growth and die-off & regrowth model(s) for each combination of nisin concentration and *Lm* strain; models for 5, 10, and 20 ppm of nisin treatments represent a combination of a Weibull inactivation submodel and a regrowth submodel (e.g., Buchanan). Bar_nl, Baranyi without lag; Buc_nl, Buchanan without lag; WeiBuc_nl, Weibull-Buchanan without lag; WeiBar_nl, Weibull-Baranyi without lag; WeiBar, Weibull-Baranyi.

[b] For a given combination of nisin concentration and *Lm* strain, the proportion of iterations in which each model is used in the simulation as determined based on the BIC model weight.

[c] The parameters of the primary growth and die-off & regrowth models. *LOG10N0,* initial level (log CFU/g); *P,* shape parameter of the Weibull inactivation submodel (no unit); *Delta,* scale parameter of the Weibull inactivation submodel (time for the first decimal reduction in population density due to antimicrobial treatments; day); *TC,* time of transition from the die-off to the regrowth phase (day); *Lag,* duration of lag phase (day); *Mumax,* maximum growth rate (day^{-1}); *LOG10Nmax,* maximum population density (log CFU/g). DIST, the parameters are characterized by a parametric distribution obtained from analyses of the data reported by Delignette-Muller et al. *(20),* Kang et al. *(40),* Tang et al. *(76),* and Chen et al. *(13)*. NA, not applicable.

scale (i.e., time of the first decimal death; *Delta*) parameters for the Weibull inactivation submodel, (ii) the time when *Lm* transits from the die-off to the regrowth phase (*TC*), (iii) the decimal log–transformed *N0* (*LOG10N0*), (iv) the lag-phase duration (*Lag*), (v) the maximum growth rate (*Mumax*), and (vi) the maximum population density (*LOG10Nmax*).

To model the die-off and/or growth kinetics of *Lm* in contaminated packages over the shelf life, one value for each die-off and/or growth associated uncertain parameters is randomly selected from the corresponding distribution and considered fixed for a given lot; these parameters include (i) the hyperparameters of *Temp* (*mTemp* and *sdTemp*), *Tmin* (*mTmin* and *sdTmin*), and $Mumax_{ref}$ ($mMumax_{ref}$ and $sdMumax_{ref}$) and (ii) the proportions of contaminated packages attributed to different serotypes (*Prop_12a, Prop_12b,* and *Prop_4b*). Within a given production lot, each contaminated package is randomly assigned a serotype, which governs the selection of the strain used for specification of the primary growth or die-off & regrowth model and the associated parameters. Values for *Temp, Tmin,* and $Mumax_{ref}$ are randomly selected from their respective distributions, conditional on the corresponding uncertain parameter values, and assigned to each contaminated package. Following the approach described in the risk assessment by the FDA and the U.S. Department of Agriculture, Food Safety and Inspection Service *(82),* the value for *Mumax* is determined based on the $Mumax_{ref}$, *Tmin,* and *Temp* values using a rearrangement of the square root model *(69)* shown in equation 1:

$$\frac{Mumax_{ref}'}{Mumax'} = \left[\frac{b(Tref - Tmin')}{b(Temp' - Tmin')}\right]^2 = \left[\frac{(25 - Tmin')}{(Temp' - Tmin')}\right]^2 \quad (1)$$

where *Tref* is the reference temperature (i.e., 25°C); *Tmin′, Temp′,* and $Mumax_{ref}'$ are the values of *Tmin, Temp,* and $Mumax_{ref}$ assigned to a given package; *Mumax′* is the value of *Mumax* calculated for the package; and *b* is the slope parameter for *Lm* on the product.

For a given contaminated package, a value for *LOG10Nmax* is randomly selected from the appropriate distribution, which differs between products with different nisin concentrations (0, 5, 10, and 20 ppm); *LOG10Nmax* values for the nisin concentrations are described by separate Weibull distributions (Table 1). Based on the experimental data for *LOG10Nmax* at the nisin concentrations reported previously *(13, 14, 40, 76),* the Weibull distribution mode across nisin concentrations is assumed to follow a nonlinear

relationship shown in equation 2:

$$Mode' = 9.12 - \left(\frac{Nisin}{18.95}\right)^{0.64} \quad (2)$$

where *Nisin* is the concentration of nisin treatments and *Mode′* is the mode of the Weibull distribution specified for a given nisin concentration. The effect of nisin concentration on the Weibull distribution standard deviation is assumed to follow a linear relationship characterized by equation 3:

$$sd' = 0.04 \times Nisin + 0.29 \quad (3)$$

where *Nisin* is the concentration of nisin treatments and *sd′* is the standard deviation of the Weibull distribution specified for a given nisin concentration. The mode and standard deviation estimated at a given nisin concentration were used to determine the shape and scale parameters needed to define the *LOG10Nmax* distribution. For die-off & regrowth models, values for *P, Delta, TC,* and *Lag* are assigned to each contaminated package according to their weights in the simulation process determined based on BIC model weights (see Table 3).

Modeling the process of *Lm* testing. Because the analytical size of food samples for *Lm* detection is generally 25 g *(81),* we modeled the process of testing a given package for presence or absence of *Lm* assuming that (i) the distribution of bacterial cells in each contaminated package is homogeneous and (ii) a 25-g portion of the product is randomly sampled from each collected package. When the number (*N*) of *Lm* cells in a contaminated package is small, it is assumed that each bacterial cell is found in one random gram of product, resulting in *N* grams of contaminated product within the package; the number of grams of uncontaminated product within a package can thus be calculated by subtracting *N* from the net weight of the product per package (*Net_Wt*). Therefore, the number of *Lm* contained in the 25-g sample (*X*) is assumed to follow a hypergeometric distribution; the probability that $X = m$ can be calculated using equation 4:

$$P(X = m) = \frac{\binom{N}{m} \cdot \binom{Net\_Wt - N}{Sample\_Size - m}}{\binom{Net\_Wt}{Sample\_Size}} \quad (4)$$

where *Sample_Size* is the analytical sample size for *Lm* detection (i.e., 25 g). For simplicity, the accuracy of the methodology for *Lm* detection was set to 100%. Consequently, the probability that a contaminated package containing *N* bacterial cells of *Lm* tests negative for *Lm* is given by:

$$P(X = 0) = \frac{\binom{Net\_Wt - N}{25}}{\binom{Net\_Wt}{25}} \quad (5)$$

The probability that a package will test positive for *Lm* is thus given by $1 - P(X = 0)$; this probability is set to 99.9% if $N > 22$ (based on $Net\_Wt = 100$ g) because the probability of detection exceeds this threshold when $N = 22$.

Modeling the sampling of cold-smoked salmon products. We assumed that (i) the probability for sampling the products (e.g., by regulatory agencies) at a processing facility is higher than that at retail stores and (ii) the probability for sampling of products collected from consumer homes is very low but still possible in cases of outbreak investigations or consumer complaints. For example, in the initial stages of outbreak investigations (before a specific product is confirmed as the outbreak source), products from multiple processors may be considered possible outbreak sources, and hence all could be subject to testing by regulatory agencies (including samples collected in consumer homes). In cases like this, even products from processors ultimately not identified as the outbreak source (e.g., because the isolates obtained from their products do not match the subtypes of the outbreak strain) may be subject to a recall action. Sampling of a production lot of cold-smoked salmon products was thus allowed to occur for product present at the processing facility, retail stores, and consumer homes, with decreasing probabilities. For simplicity, it is assumed that (i) the probability that sampling will occur on a given day is the same for each day within a given stage (i.e., the facility, retail stores, or consumer homes), and (ii) the probability that sampling will occur on a given day at retail stores is fivefold lower than that at the facility, whereas the probability that sampling will occur on a given day at consumer homes is fivefold lower than that at retail stores (baseline scenario). Sampling probability ratios are modeled as a uniform distribution with a minimum of 1 and a maximum of 10 (Table 1). The ratio of the probability of sampling between the facility and retail stores and between retail stores and consumer homes (*Sampling_R*; Table 1) is used to determine a probability distribution of sampling time, based on which 10,000 sampling days are randomly selected for each given lot and a binary result (at least one package tests positive for *Lm* versus no package tests positive for *Lm*) is determined for each sampling. The RR risk for a given lot is calculated by dividing the number of samplings that lead to *Lm*-positive tests by the total number of samplings.

Sensitivity analysis. One-at-a-time sensitivity analysis was performed to test the sensitivity of RR risks to each of the variable parameters by running the model under various scenarios (i.e., with various parameter settings; see Supplemental Table S1 for details). The parameter space of each variable parameter being tested was divided into 1,000 equally probable intervals, and a value was randomly drawn from each of the intervals, leading to a collection of 1,000 parameter values. Each of the 1,000 values was randomly assigned to one production lot and fixed for all packages in the given lot. The Spearman rank correlation coefficient (SRCC) was calculated to infer the correlation between the parameter and RR risk using the stats v. 3.5.2 package *(70)*. The resulting distribution of RR risks was compared with the distribution under the baseline scenario where uncertain parameters were set to baseline values (Table S1).

The uncertain parameters *Prev* and *Sampling_R* are not related to the rest of the parameters and were thus tested independently using the approach described above for the variable parameters. The other uncertain parameters were divided into five groups based on inherent dependency, and parameters within the same group were tested simultaneously: (i) *mTemp* and *sdTemp* (the hyperparameters of *Temp*), (ii) *mTmin* and *sdTmin* (the hyperparameters of *Tmin*), (iii) *mLnN0* and *sdLnN0* (the hyperparameters of *N0*), (iv) $mMumax_{ref}$ and $sdMumax_{ref}$ (the hyperparameters of $Mumax_{ref}$), and (v) *Prop_12a, Prop_12b,* and *Prop_4b* (proportions with which each serotype contaminates a given lot). When the model was run to test the sensitivity of RR risks to multiple parameters simultaneously, all parameters were sampled from their respective parameter space through Latin hypercube sampling, using the lhs v. 1.0.1 package *(10),* resulting in 1,000 combinations of parameter values (Table S1). Each combination was assigned to one production lot, and the RR risk of the specific production lot was determined. The partial rank

correlation coefficient (PRCC) *(41)* was used to characterize the correlation between each of the parameters and the RR risk while controlling the other variables in the same group, using the epiR v. 1.0.13 package *(74)*. The resulting distributions of RR risks were compared with the distribution provided by the baseline scenario with uncertainty parameters set to baseline values (Table S1).

Scenario analysis. For scenario (what-if) analyses, alternative scenarios representing potential interventions to reduce RR risks were defined, and the model was run under specific parameter settings that mimic each of the scenarios (Table S1). The efficacy of the interventions for reducing RR risks was assessed by comparing the RR risks predicted by running the model under the alternative scenarios and the baseline scenario (see Table S1). Alternative scenarios assessed were (i) products treated with 5, 10, and 20 ppm of nisin before vacuum packing; (ii) all products stored and distributed at <5 or <6°C (which could be achieved by use of a time-temperature indicator *(54)* attached to each package); (iii) products reformulated with bacteriostatic growth inhibitors (i.e., a combination of 2% potassium lactate and 0.14% sodium diacetate) that are assumed to reduce *Mumax* (day^{-1}) and *LOG10Nmax* (log CFU per gram) by 0.2 and 1.3, respectively, and to extend *Lag* (day) by 21.4 *(40)*; and (iv) the prevalence of *Lm* reduced by 50% (e.g., through stringent implementation of pathogen environmental monitoring programs, good manufacturing practices, and sanitation standard operation procedures) *(66)*.

Assessment of model performance for predicting Lm die-off and growth on cold-smoked salmon. To the best of our knowledge, data enabling the direct validation of RR risks are not yet available; hence, we assessed our model only with regard to its ability to predict die-off and/or growth of *Lm* on cold-smoked salmon treated with various nisin concentrations, using data from a challenge study of *Lm* on cold-smoked salmon *(13)*. This study is not completely independent from the model because the data for day 30 *Lm* levels were included in the data used to characterize the parametric distributions for *LOG10Nmax*. However, the data for day 15 *Lm* levels for untreated and nisin-treated samples were not included in the model development and were thus used to assess the model performance. The model was run with parameters adjusted to mimic the experiment settings (e.g., inoculum level and storage temperature) used to generate the experimental data reported in the study. Simulated day 15 *Lm* data generated for products treated with 0 and 20 ppm of nisin were compared with the experimental data for untreated and nisin-treated samples, respectively. To account for the variation in *Lm* enumeration due to uncontrollable experimental factors, an error term is associated with the primary growth and die-off & regrowth models. According to Delignette-Muller et al. *(20),* this error term is assumed to follow a normal distribution with a mean of 0 and a standard deviation of sd_{error}, where the natural log–transformed sd_{error} is assumed to follow a normal distribution with a mean of −1.20 and a standard deviation of 0.0185. For each comparison, the proportion of the simulated data that fall within the range of the experimental data was calculated, and the Mann-Whitney U test was used to determine whether the medians of the simulated and the experimental data differed from each other at $\alpha = 0.05$ (stats v. 4.0.2 package).

RESULTS

Baseline prediction of the RR risk for cold-smoked salmon products. In the 3R model, we consider RR risks as the likelihood of having at least one *Lm*-positive sample given that a set number of samples are tested for a given lot. The RR risk predicted through the 3R model is presented as a distribution and summarized using the median and the 95% credible interval (CI). In the second-order Monte Carlo simulation framework used for our 3R model, variability is assumed to occur in a given lot across packages with respect to certain product and *Lm* growth parameters, whereas uncertainty is assumed to be present across lots. Because RR risks are lot-level predictions (i.e., a value for RR risk is associated with a given lot rather than a given package of the product), they are calculated while accounting for the variability among packages within a given lot. Consequently, the distribution of RR risks output from the model is mainly reflective of the uncertainty dimension of the framework. This risk outcome presentation differs from that of outcomes of most public health risk assessments conducted with second-order Monte Carlo simulations *(64, 66, 83),* which typically consist of distributions that characterize both variability and uncertainty. Under the baseline scenario, the median RR risk was 0.333 (95% CI: 0.288, 0.384), 0.183 (95% CI: 0.156, 0.215), and 0.040 (95% CI: 0.032, 0.048) for $n = 10$, $n = 5$, and $n = 1$ sampling schemes, respectively (Fig. S1). These predicted RR risks are for production lots with an *Lm* prevalence of 4% and no interventions implemented, which may not be representative for contemporary cold-smoked salmon products across markets and countries. Therefore, these data should not be interpreted as 33.3% (or 18.3 or 4%) of the products in the market should be recalled or otherwise handled assuming *Lm* contamination. Rather, our results suggest that high RR risks should be expected for products with a reasonably high contamination frequency (e.g., smoked seafoods) and no appropriate control strategies, especially when large numbers of samples are collected.

Model performance for predicting *Lm* die-off and growth on cold-smoked salmon. A challenge study of *Lm* on cold-smoked salmon treated with 0 or 25 ppm of nisin performed by Chen et al. *(13)* provided day 15 *Lm* enumeration data for salmon stored at 7°C. These data were used to assess the performance of the 3R model with regard to predicting *Lm* die-off and/or growth kinetics on contaminated products. The comparisons of the empirical distributions between the simulated ($n = 100$) and experimental ($n = 24$) data for *Lm* levels is shown in Figure 2 (see Table S2 for detailed statistics). For cold-smoked salmon products without nisin treatments, the experimental *Lm* levels were 8.17 to 9.27 log CFU/g at day 15, and the simulated levels for day 15 were 6.59 to 9.71 log CFU/g, with 71% of the data points falling within the range of the experimental data. The Mann-Whitney U test indicated no significant difference in median between the experimental and the simulated data ($P = 0.179$). For cold-smoked salmon products with nisin treatments, the experimental data for *Lm* on salmon treated with 25 ppm of nisin was compared with the simulated data for *Lm* on salmon treated with 20 ppm of nisin because this is the highest nisin concentration that can be specified in the

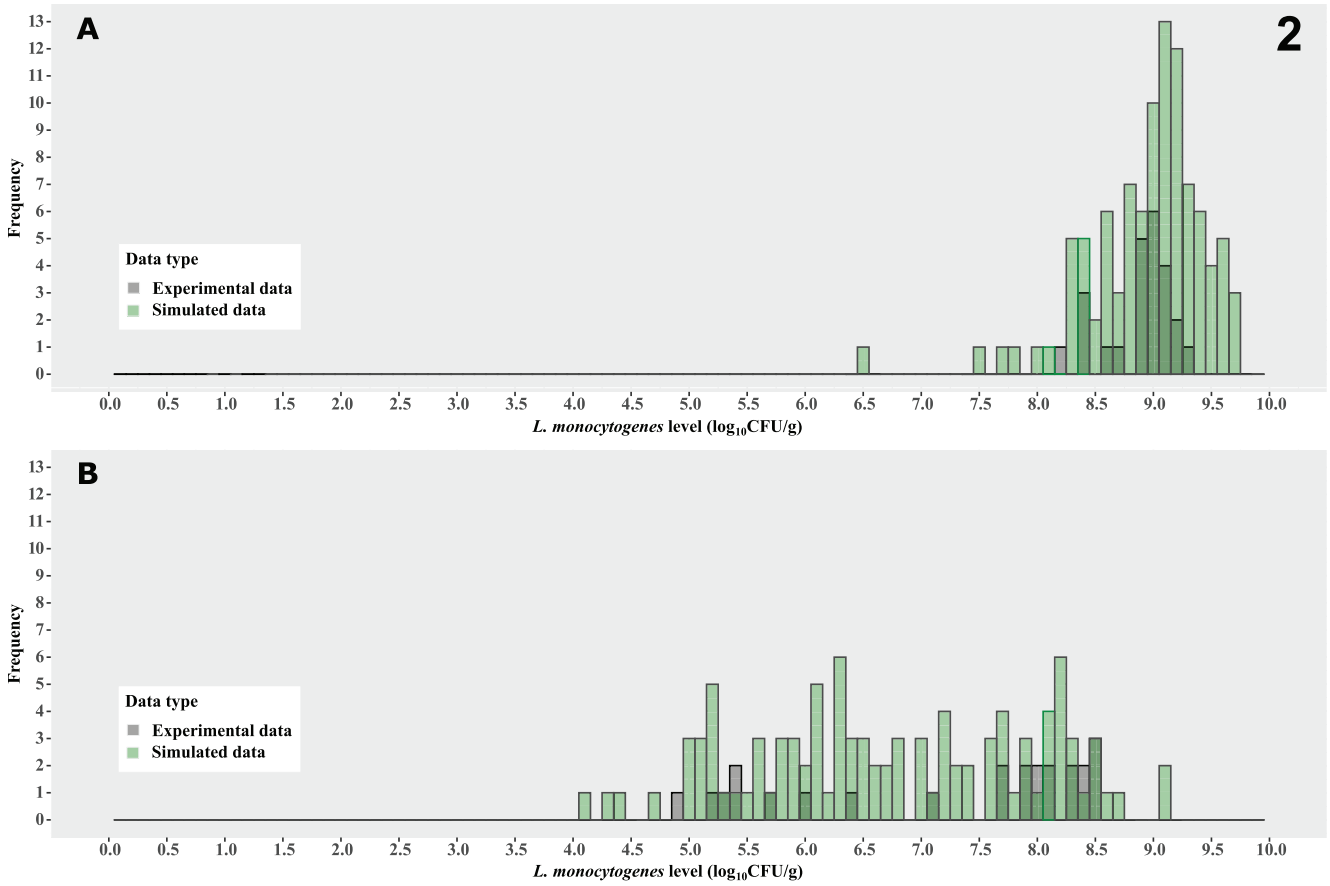

FIGURE 2. *Comparison between the simulated levels of* Lm *(log CFU/g) on cold-smoked salmon and the experimental data of Chen et al. (13). (A) Simulated and experimental* Lm *levels on untreated salmon after 15 days of storage at 7°C; (B) simulated* Lm *levels on salmon treated with 20 ppm of nisin and experimental* Lm *levels on salmon treated with 25 ppm of nisin after 15 days of storage at 7°C.*

current version of the 3R model. A total of 92% of the simulated data (day 15 levels of 4.05 to 9.07 log CFU/g) were within the range of the experimental data (day 15 levels of 4.88 to 8.52 log CFU/g); the Mann-Whitney U test indicated that the medians of the experimental and simulated data were not significantly different ($P = 0.07$). Although a weakness of this method is that model predictions for 20 ppm were assessed with experimental data for 25 ppm, the impact of this approach is likely to be limited relative to variability of nisin concentrations expected to be present in commercial products. Kang et al. *(40)* reported that the dose-dependent increase in efficacy of nisin against *Lm* slowed down as the nisin concentration increased from 0 to 20 ppm. In their study, none of the relevant die-off and growth parameters differed significantly between 10 and 20 ppm of nisin, further supporting our assumption that differences between *Lm* levels on salmon treated with 20 and 25 ppm of nisin would be negligible. Overall, our results support the ability of the 3R model to provide reasonable estimates for *Lm* levels on both untreated and nisin-treated cold-smoked salmon.

Sensitivity analysis. The sensitivity of RR risks to each of the variable parameters was assessed using the one-at-a-time approach by running the models under different scenarios that allowed us to assess the impact of (i) storage temperature variability (Var_Temp), (ii) nominal minimum growth temperature variability (Var_Tmin), (iii) initial contamination level variability (Var_N0) (iv) reference temperature maximum growth rate variability (Var_Mu-max$_{ref}$), and (v) maximum population density variability (Var_LOG10Nmax) (see Table S1 for detailed parameter settings). The medians and 95% CIs for the empirical distributions of the predicted RR risk provided by running the model under scenarios specified for the various variable parameters were not different from those of the baseline scenario with uncertain parameters set to their baseline value (Figs. 3 and S2). However, the SRCC between the RR risk and the variable parameters (Figs. 4 and S3) revealed that RR risk was positively correlated with initial contamination level ($P < 0.001$), maximum growth rate at the reference temperature ($P < 0.001$), and storage temperature ($P < 0.001$) and negatively correlated with nominal minimum growth temperature ($P < 0.001$); maximum population density was not correlated with RR risk. According to Cohen's standard *(16, 17),* the effect size was medium for initial contamination level (SRCC = 0.405) and maximum growth at the reference temperature (SRCC = 0.275) and small for storage temperature (SRCC = 0.177) and nominal minimum growth temperature (SRCC = –0.169).

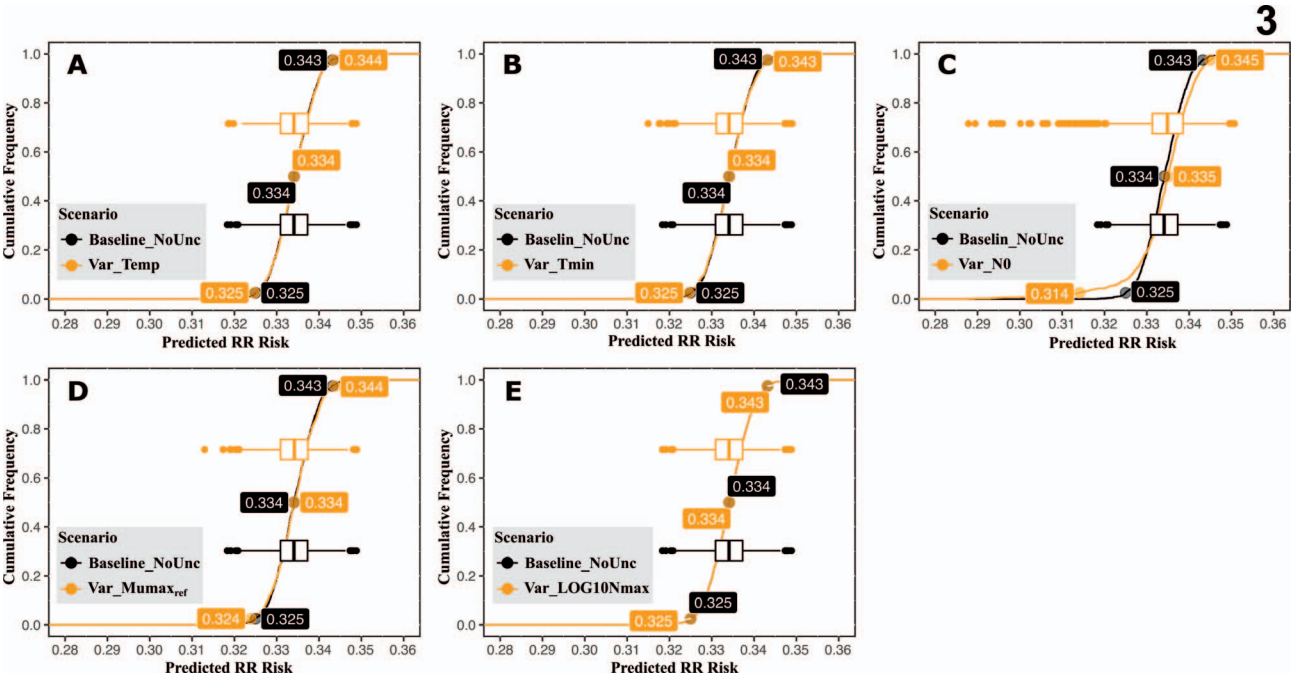

FIGURE 3. *Empirical cumulative distribution functions (ECDFs) and the corresponding boxplots of the predicted regulatory and recall (RR) risk obtained by running the model under the baseline scenario with uncertain parameters set to their baseline value (Basline_NoUnc) and alternative scenarios specified in the sensitivity analysis for assessing the impact of (A) storage temperature variability (Var_Temp), (B) nominal minimum growth temperature variability (Var_Tmin), (C) initial contamination level variability (Var_N0), (D) reference temperature maximum growth rate variability (Var_Mumax$_{ref}$), and (E) maximum population density variability (Var_LOG10max). Within each panel, medians of the distributions and the upper and lower bounds of the 95% credible intervals are plotted on the ECDF as shaded circles and noted by numbers next to the circles. For each of the boxplots, the box encompasses the region from the first to the third quartile, with the median denoted by the line in the box. The upper whisker extends from the upper end of the box to the largest value no further than 1.5 times the interquartile range, and the lower whisker extends from the lower end of the box to the smallest value no further than 1.5 times the interquartile range. Data points beyond the end of the whiskers are plotted as dots.*

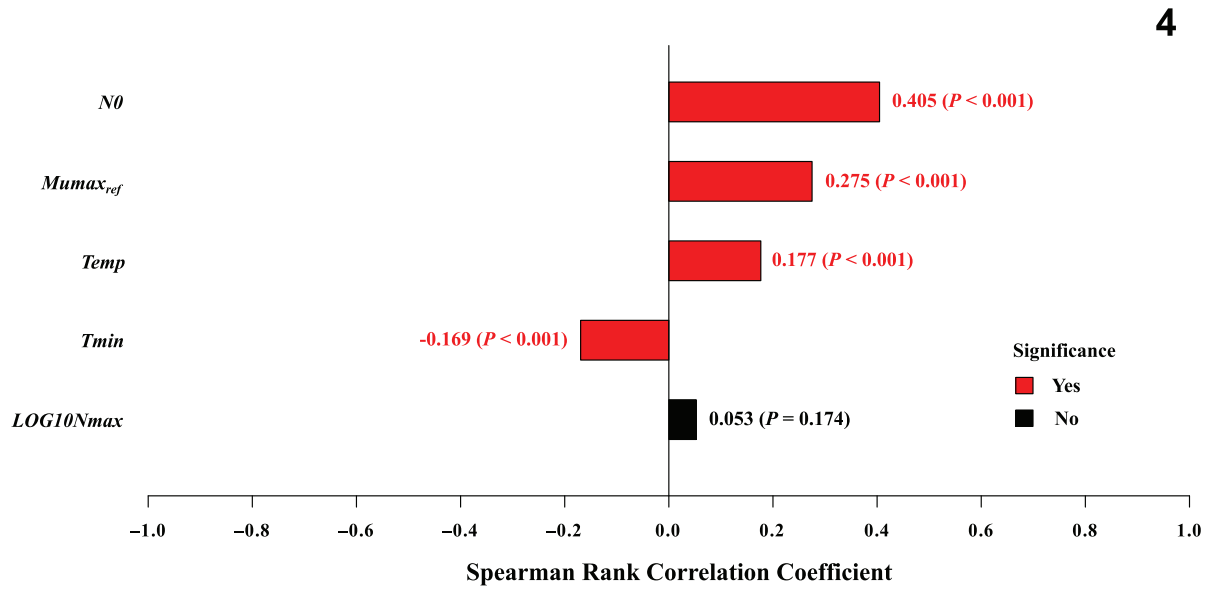

FIGURE 4. *Sensitivity of regulatory and recall (RR) risks to the model variable parameters: (i) storage temperature (*Temp*); (ii) nominal minimum growth temperature (*Tmin*); (iii) initial contamination level (*N0*); (iv) maximum growth rate at the reference temperature (*Mumax$_{ref}$*); and (v) maximum population density (*LOG10Nmax*). The Spearman rank correlation coefficients between each parameter and the predicted RR risk are presented as the horizontal bars with the numbers and the associated* P *values shown next to the respective bars. Positive and negative values indicate positive and negative correlations, respectively.*

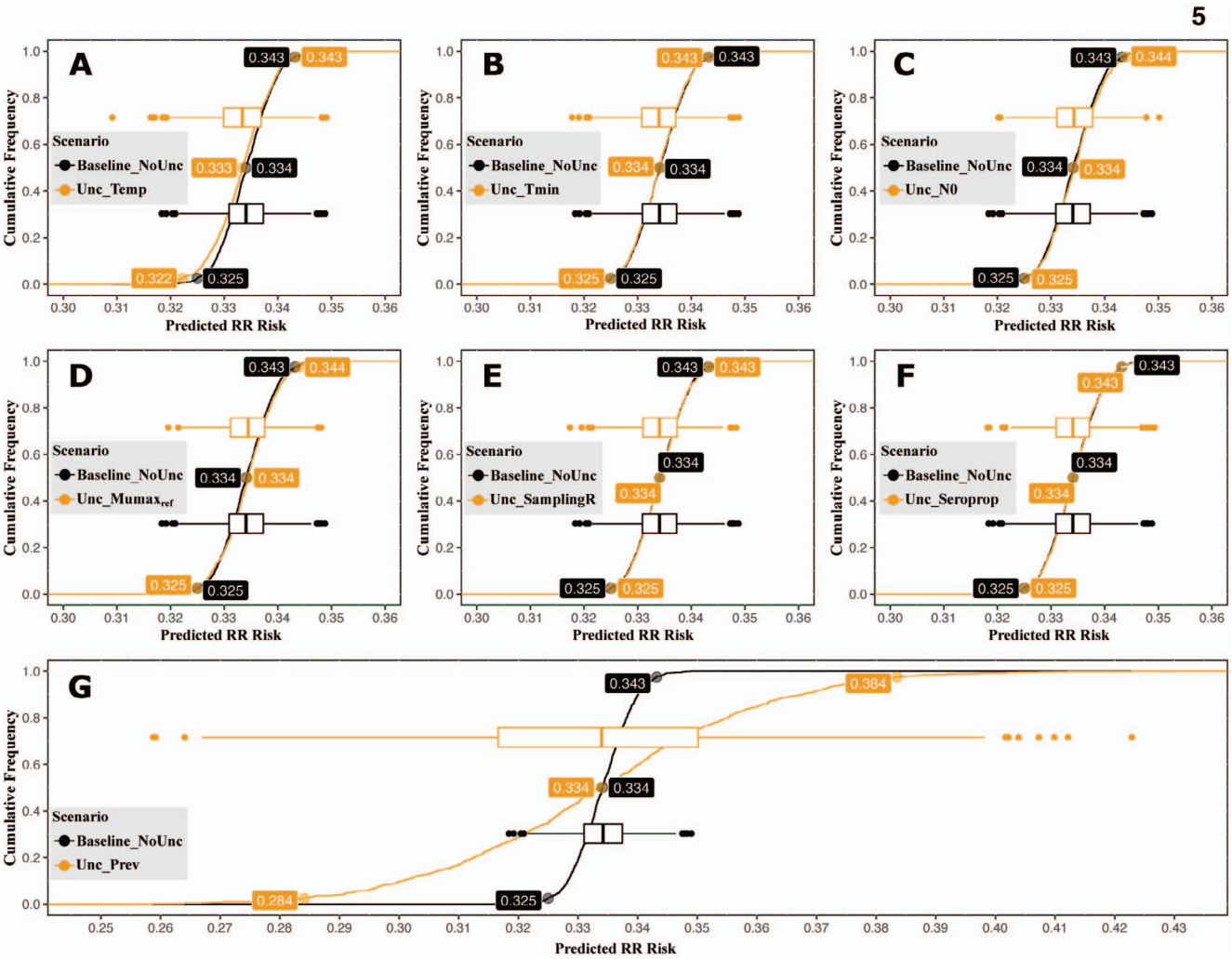

FIGURE 5. *Empirical cumulative distribution functions (ECDFs) and the corresponding boxplots of predicted regulatory and recall (RR) risk obtained by running the model under the baseline scenario with uncertain parameters set to their baseline value (Baseline_NoUnc) and alternative scenarios specified in the sensitivity analysis for assessing the uncertainty of (A) mean and standard deviation of storage temperature (Unc_Temp); (B) mean and standard deviation of nominal minimum growth temperature (Unc_Tmin); (C) mean and standard deviation of natural log–transformed initial contamination level (Unc_N0); (D) mean and standard deviation of reference temperature maximum growth rate (Unc_Mumax$_{ref}$); (E) ratio of sampling likelihood at various stages (Unc_SamplingR); (F) proportion of contaminated packages attributed to the three serotypes (Unc_SeroProp); and (G)* Lm *prevalence (Unc_Prev). Within each panel, medians of the distributions and the upper and lower bounds of the 95% confidence intervals are plotted on the ECDF as shaded circles and noted by the numbers next to the circles. For each of the boxplots, the box encompasses the region from the first to the third quartile, with the median denoted by the line in the box. The upper whisker extends from the upper end of the box to the largest value no further than 1.5 times the interquartile range, and the lower whisker extends from the lower end of the box to the smallest value no further than 1.5 times the interquartile range. Data points beyond the end of the whiskers are plotted as dots.*

To assess the sensitivity of RR risks to the various uncertain parameters, seven scenarios were specified for testing the uncertainty of (i) mean and standard deviation for storage temperature (Unc_Temp), (ii) mean and standard deviation of the distribution of nominal minimum growth temperature (Unc_Tmin), (iii) mean and standard deviation of the distribution of natural log–transformed initial contamination level (Unc_N0), (iv) mean and standard deviation of the distribution of maximum growth rate at the reference temperature (Unc_Mumax$_{ref}$), (v) *Lm* prevalence (Unc_Prev), (vi) ratio of sampling likelihood between stages (Unc_SamplingR), and (vii) proportion of contaminated packages attributed to the three serotypes (Unc_SeroProp) (see Table S1 for detailed parameter settings). In these analyses, variation in prevalence contributes a considerably higher variation in the predicted RR risk (95% CI: 0.285, 0.386) than does the variation under the baseline scenario with uncertain parameters set to their baseline values (Figs. 5 and S4). Consistent with these findings, RR risk was positively correlated with *Lm* prevalence ($P < 0.001$) with a large effect size (SRCC = 0.981; Figs. 6 and S5). This indicates that the uncertainty of *Lm* prevalence contributed significantly to the variation of the predicted RR risk; thus, a good estimation of this parameter is important for making precise predictions. Other sources of uncertainty that contributed significantly to the variation of the predicted RR risk (Figs. 6 and S5) include mean of the distribution of storage temperature (*P*

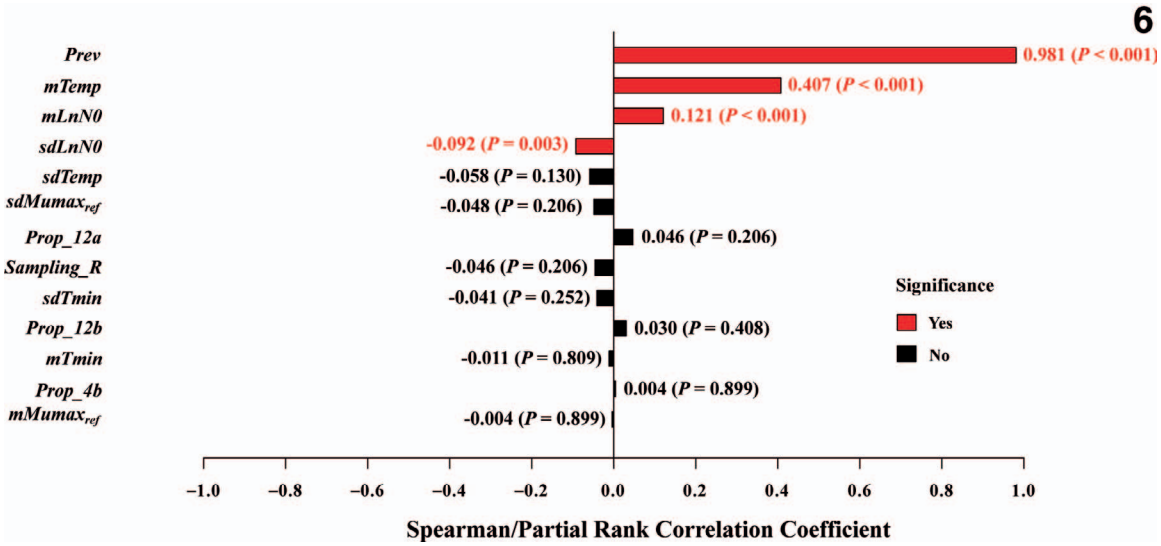

FIGURE 6. *Sensitivity of regulatory and recall (RR) risks to the model uncertain parameters: (i) mean (*mTemp*) and standard deviation (*sdTemp*) of storage temperature; (ii) mean (*mTmin*) and standard deviation (*sdTmin*) of nominal minimum growth temperature; (iii) mean (*mLnN0*) and standard deviation (*sdLnN0*) of natural log–transformed initial contamination level; (iv) mean (*$mMumax_{ref}$*) and standard deviation (*$sdMumax_{ref}$*) of reference temperature maximum growth rate; (v) ratio of sampling likelihood at various stages (*Sampling_R*); (vi) proportion of contaminated packages attributed to the three serotypes (*Prop_12a, Prop_12b, *and* Prop_4b*); and (vii)* Lm *prevalence (*Prev*). The Spearman rank correlation coefficients (for parameters* Prev *and* Sampling_R*) or the partial rank correlation coefficients (for parameters* mTemp, sdTemp, mTmin, sdTmin, mLnN0, sdLnN0, mMumax, sdMumax, Prop_12a, Prop_12b, *and* Prop_4b*) between the parameters and the predicted RR risk are presented as horizontal bars with the numbers and the associated* P *values shown next to the respective bars. Positive and negative values indicate positive and negative correlations, respectively.*

< 0.001) and mean ($P < 0.001$) and standard deviation ($P = 0.008$) of the distribution of natural log–transformed initial contamination level. The effect size of the correlation with RR risks was medium for mean of the distribution of storage temperature (PRCC = 0.407) and small for mean (PRCC = 0.121) and standard deviation (PRCC = –0.092) of the distribution of natural log–transformed initial contamination level *(16, 17)*. The uncertainties associated with the characteristics of *Lm,* including the parameters associated with nominal minimum growth temperature, maximum growth rate at the reference temperature, and *Lm* serotype, did not significantly contribute to the variation in the predicted RR risk. The ratio of sampling likelihood between the facility and retail stores (and between retail stores and consumer homes) was not significantly correlated with RR risk. This suggests that the impact of time (and location) of sample collection on RR risks is limited; thus, reliable data on regulatory sample collection practices is not essential for the type of 3R model reported here.

Scenario analysis. Seven scenarios with parameter settings specified to mimic a variety of interventions were used to assess the effectiveness in reducing RR risks of (i) treatment with 5 ppm of nisin (WI_NT5), (ii) treatment with 10 ppm of nisin (WI_NT10), (iii) treatment with 20 ppm of nisin (WI_NT20), (iv) controlling temperature to <6°C (WI_TC6), (v) controlling temperature to <5°C (WI_TC5), (vi) treatment with bacteriostatic growth inhibitors (WI_GI), and (vii) a 50% reduction in *Lm* prevalence (WI_Prev50) (see Table S1 for detailed parameter settings). Nisin treatments drastically reduced RR risks compared with the baseline scenario (without nisin treatments), and the effectiveness for reducing RR risks increased with increased nisin concentration (Fig. 7A and 7C). Treatment of the products with 5 ppm of nisin resulted in a reduction in the predicted RR risk from 0.333 (95% CI: 0.288, 0.384) to 0.109 (95% CI: 0.074, 0.146). When the nisin concentration was increased to 20 ppm, the predicted RR risk was further lowered to 0.017 (95% CI: 0.001, 0.033). Reduction of the prevalence of *Lm* contamination among finished products by 50% also was an effective strategy for reducing RR risks (Fig. 7A and 7C); under this scenario, the predicted RR risk was 0.182 (95% CI: 0.153, 0.213). In comparison, reformulation of the products with bacteriostatic growth inhibitors (a combination of 2% potassium lactate and 0.14% sodium diacetate) led to a considerably lower reduction of the predicted RR risk. With bacteriostatic growth inhibitors assumed to result in a 0.2-day^{-1} reduction in maximum growth rate, a 1.3-log reduction in maximum population density, and a 21.4-day extension in lag phase, the predicted RR risk was reduced to only 0.313 (95% CI: 0.268, 0.367; Fig. 7A and 7C). Assuring appropriate cold storage of all products (no products exposed to a storage temperature >6 or >5°C) did not reduce RR risks (Fig. 7B and 7D).

DISCUSSION

Smoked seafood is an RTE food that historically has a high frequency of recalls *(12, 71, 79)*. Although various growth models and public health risk assessments for *Lm* in smoked seafood have been developed *(49, 50, 65, 66, 82),* selection of appropriate interventions to implement at the production level remains a challenge. This challenge is

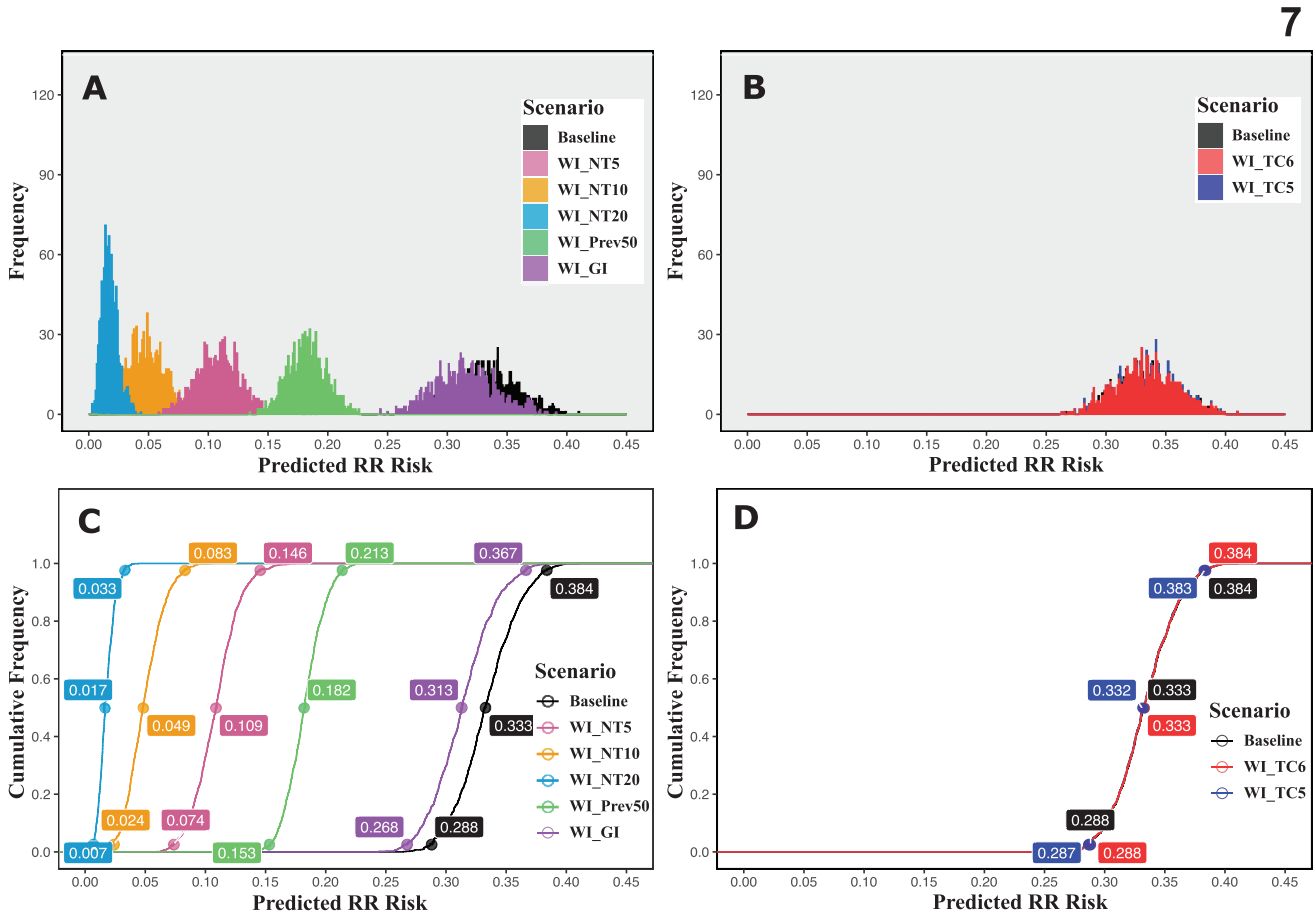

FIGURE 7. *Comparison of the predicted regulatory and recall (RR) risk for cold-smoked salmon products produced under the baseline scenario and alternative scenarios. (A) Histograms of the predicted RR risk of the products produced under (i) the baseline scenario (Baseline), (ii) treatment with 5 ppm of nisin (WI_NT5), (iii) treatment with 10 ppm of nisin (WI_NT10), (iv) treatment with 20 ppm of nisin (WI_NT20), (v) reformulation with growth inhibitors (2% potassium lactate and 0.14% sodium diacetate; WI_GI), and (vi) a 50% reduction in the prevalence of* Lm *contamination (WI_Prev50). (B) Histograms of the predicted RR risk of the products produced under the baseline scenario (Baseline) or with temperature controls (i.e., removing all products that have been stored at >6°C [WI_TC6] or 5°C [WI_TC5]). (C) Empirical cumulative distribution functions (ECDFs) of the predicted RR risk of the products produced under the scenarios presented in panel A. Medians of the distributions and the upper and lower bounds of the 95% credible intervals are plotted on the ECDFs as shaded circles and noted by the numbers next to the circles. (D) ECDFs of the predicted RR risk of the products produced under the scenarios presented in panel B. Medians of the distributions and the upper and lower bounds of the 95% credible intervals are plotted on the ECDFs as shaded circles and noted by the numbers next to the circles. Temperature control scenarios are shown separately in panels B and D for better visualization.*

compounded by the fact that some interventions have been reported in the peer-reviewed literature, some are marketed by commercial entities, and some are suggested by customers or regulatory agencies. In addition to the challenge of selecting specific interventions, the mechanisms of available *Lm* interventions must be considered; some interventions (i) reduce prevalence and levels of *Lm,* (ii) reduce or prevent growth, or (iii) achieve both reduced prevalence (and levels) and reduced growth. To improve the ability of producers to select appropriate interventions, we developed the 3R model, a decision support tool that can help with *Lm* risk management and selection of interventions. Distinct from the previous risk assessment models, the 3R model focuses on assessing the impact of interventions on the risk of food recalls or other regulatory consequences due to *Lm* contamination; however, both RR risk and public health risk models should be used to support decision making. We have detailed a roadmap that illustrates how existing public health risk assessments and growth models provide a valuable starting point for developing RR risk models. We found (i) that accurate data on product temperature and *Lm* prevalence and initial levels are needed for reliable RR risk models and (ii) that nisin treatments are the most effective interventions for reducing RR risks and *Lm* interventions that reduce only prevalence are less effective but still lead to more effective RR risk reductions than do interventions that only retard growth. The RR risk modeling approach detailed here should be easily applicable to other foods (e.g., produce) for which improved decision making on pathogen interventions is desired.

Existing public health risk assessments and growth models provide a valuable starting point for developing RR risk models. One advantage of using cold-smoked

salmon as a model product to develop the 3R model is that a large number of studies and original data are available, which provide or can be used to estimate values or distributions of model parameters specific for this product, as recommended by the Codex Alimentarius Commission *(15)* and supported by Pradhan et al. *(68)*. In the present study, the parameters used to model the die-off and growth kinetics of *Lm* on contaminated products were characterized using data specifically generated for *Lm* on cold-smoked salmon with various nisin treatments *(40)*. To further improve the estimation of *Lm* levels on contaminated products across days, each die-off–growth curve was fit with either five primary growth or five die-off & regrowth models to ensure that the best-fit model and its associated parameters were used for modeling *Lm* die-off and/or growth kinetics. Similar to previous studies *(8, 20, 66, 68, 82),* the square root model *(69)* was applied to model the effect of temperature on the maximum growth rate of *Lm*. Although various other environmental factors or product characteristics can affect the maximum growth rate of *Lm,* including pH, water-phase salt content, phenolic concentration, nitrites, and dissolved CO_2 *(18, 49),* we did not adjust growth parameters based on these factors because (i) they have been insufficiently characterized to infer appropriate distributions *(20)* and (ii) their effects are accounted for through the variability and uncertainty associated with the maximum growth rate at the reference temperature. Another simplification made for the model was the constant storage temperature for a given package across stages (i.e., the facility, retail stores, and consumer homes). Although growth of *Lm* on cold-smoked salmon under varying temperature conditions has been modeled previously using the DMS model *(66),* we made the simplifying assumption of a constant storage temperature, at least in part because the data and tools were not available to allow for temperature adjustments of die-off and growth parameters required for the primary growth models and the Weibull submodel for microbial inactivation. This simplification may underestimate the temperature at the consumer stage, which is associated with a higher likelihood of temperature abuse. However, underestimation of the consumer temperature is not likely to have a substantial impact on predicting RR risks and the reduction in RR risks achieved by various interventions. First, the 3R model considers that the probability that a given package to be tested is positive for *Lm* is ca. 1 when the contamination level is >22 CFU per package (assuming a net weight of 100 g and a sample size of 25 g). Given that the baseline temperature distribution centers at 4.4°C, sufficient *Lm* growth to achieve this contamination level is likely (even with a starting inoculum of one cell per package) because the consumer stage is assumed to start 40 days after the end of production. Second, the probability of sampling at the facility and retail stores is considerably higher than that of sampling at consumer homes; hence, underestimation of growth at the consumer stage is likely to have limited impact on RR risks.

Similar to previous risk assessments *(20, 64, 66, 83),* a second-order Monte Carlo simulation framework *(27, 56, 85),* which enables separate analyses of variability and uncertainty, was used for the 3R model, allowing for variation of uncertain parameters across production lots and variable parameters across product packages within a lot. In the simulation process, we included both variable and uncertain components for various factors (storage temperature, maximum growth rate at the reference temperature, initial contamination level, and nominal minimum growth temperature) associated with a given package when existing data and tools allowed for reliable characterization of the respective distributions. Because *Lm* prevalence is typically associated with a given lot instead of a given package, prevalence was treated as a lot-level parameter, such that each lot was assigned a single value for *Lm* prevalence, which was allowed to differ across lots. The variation of *Lm* prevalence across lots was deemed uncertain at least partially because the lack of sufficient data to derive a distribution that characterizes variability. Thus, the distribution of prevalence was inferred based on a non–data-based prior suggested by Miconnet et al. *(52)* and the prevalence of *Lm* in smoked seafood products in the United States reported in only three studies *(31, 42, 77)*. Therefore, future studies on variability of *Lm* prevalence, among other critical lot-level factors, will allow further improvements of the 3R model. The RR risk predicted under the baseline scenario highly depends on the number of products sampled (our baseline scenario assumed sampling of 10 products per lot), a number that end users may want to modify based on sampling schemes expected for their products. The 3R model assesses the RR risk of a given production lot, with a lot designated as being recalled or triggering other regulatory consequences when at least one package tests positive for *Lm* and regardless of the total number of packages that test positive. The actual levels of *Lm,* when above the detection threshold (0.04 CFU/g), are not likely to affect the RR risk. In our 3R model, the RR risk is calculated for a given production lot, which is different from the approach used for public health risk assessments, which typically calculate risks per serving or population denominator. Therefore, although both variability and uncertainty have been included in the 3R model, for some factors the 95% CI reported for the RR risk does not reflect the variability among product packages because RR risk is a lot-level risk outcome. This situation illustrates the challenge of separately assessing variability and uncertainty associated with lot-level risk outcomes as compared with package- or serving-level risk outcomes (e.g., the risk of human listeriosis), which should represent a focus for future studies. In the sensitivity analysis conducted to identify variable and uncertain parameters important for predicting RR risks, the effect size for parameters was represented by SRCC or PRCC, nonparametric measures for nonlinear but monotonic relationships *(46)* that have been used in sensitivity analyses in multiple risk assessments *(67, 78, 80, 87)*. Although an analysis of variance (ANOVA) method *(66)* and Sobol sensitivity indices *(84)* have been used for these types of analyses and can account for interactions between model parameters *(53),* their implementation requires an unrealistic setting for the 3R model (i.e., all packages within the same production lot share same values

for the variable parameters); we thus selected rank-based methods for sensitivity analyses conducted here.

Sensitivity analyses suggest that accurate data on product temperature and *Lm* prevalence and initial levels are needed for reliable RR risk models. Sensitivity analysis of the uncertain parameters revealed that parameters related to product temperature and *Lm* prevalence and initial levels had a significant impact on the RR risk. Among these parameters, prevalence of *Lm* on cold-smoked salmon products had the largest impact on the RR risk followed by initial levels of *Lm* and product temperature. These results support the assumption that additional data on the prevalence of *Lm* is the most important factor for improving the prediction of RR risks; more extensive data on temperature and initial contamination levels also will substantially increase the accuracy of model predictions. The uncertainties associated with the maximum growth rate and nominal minimum growth temperature of *Lm* and the proportions of contaminated products attributed to various serotypes did not significantly contribute to the variation in the predicted RR risk, suggesting that the 3R model requires limited additional data collection with respect to these parameters.

Sensitivity analyses also revealed that four variable parameters had a significant impact on the RR risk, including two parameters linked to characteristics of the contaminated product (storage temperature and initial contamination level) and two growth parameters (maximum growth rate at the reference temperature and nominal minimum growth temperature). The initial *Lm* contamination level was positively correlated with the RR risk, with the highest effect size among the variable parameters. In previous studies, researchers have also identified the initial *Lm* contamination level as an important variable that affects listeriosis risks due to consumption of contaminated food products, including cold-smoked salmon *(66),* frozen vegetables *(88),* and RTE deli products *(28)*. As a result, interventions that target a reduction in the initial *Lm* contamination level may be effective for reducing RR risks. The predicted RR risk increased with the increase in the maximum growth rate of *Lm* and the increase in storage temperature for the products, indicating higher RR risks for cold-smoked salmon products stored in environments that facilitate the growth of *Lm,* such as environments with high temperatures. A decrease in the nominal minimum growth temperature of *Lm* also led to an increase in the predicted RR risk, suggesting that contamination with *Lm* isolates that grow faster at refrigeration temperatures increased RR risks. These results are consistent with those of a previous quantitative risk assessment of *Lm* on French cold-smoked salmon products, in which an ANOVA-based approach was used to rank the sensitivity of predicted *Lm* levels in a contaminated serving to various model parameters *(66)*. Even with a different model outcome and methodology for the sensitivity analysis, those researchers also concluded that maximum growth rate, nominal minimum growth temperature, and product temperature were significant parameters *(66)*. Therefore, these parameters were consistently identified as additional targets for interventions, even if the relative impact may differ depending on the types of risk outcomes assessed (e.g., public health risk versus RR risk), as further discussed in the following section. The fact that maximum growth rate and nominal minimum growth temperature were deemed appropriate targets for interventions but not targets for additional data collection or research (because we found an impact of the variability but not the uncertainty associated with these two factors) demonstrates the merit of the separate modeling of variability and uncertainty, which can be achieved using the second-order Monte Carlo simulation framework as in our 3R model and previous risk assessment models.

Although nisin treatments are the most effective *Lm* interventions for reducing RR risks, interventions that reduce only *Lm* prevalence are less effective but still lead to more effective RR risk reductions than do interventions that only retard growth. As an FDA-approved natural antimicrobial, nisin has been extensively studied for its efficacy for reducing *Lm* levels on cold-smoked salmon *(40, 57, 60, 76, 86)*. However, the potential of nisin to reduce the risk of listeriosis or of regulatory consequences (e.g., recalls) associated with cold-smoked salmon products remained to be explored. Based on our scenario analysis, nisin treatments drastically reduced the RR risk in a concentration-dependent manner (i.e., higher nisin concentrations lead to more pronounced reductions in RR risk) and are the most effective intervention for reducing RR risks. The effectiveness of the nisin treatments for reducing RR risks can be attributed to the fact that these treatments reduced both (i) the total number of the contaminated packages and (ii) the initial *Lm* contamination levels in those packages that remained contaminated. Improved accuracy of the predicted effect of various nisin concentrations on RR risks could be achieved by addressing some simplifying assumptions that had to be made for our model due to the unavailability of the data that would be needed to assess all complexities of nisin-mediated *Lm* control. For example, the underlying primary growth and die-off & regrowth models do not account for the Jameson effect (suppression of *Lm* growth by competitive microbiota present on salmon), which has been included in previous studies that predicted *Lm* growth in seafood-associated products *(48, 51)*. Another simplification related to the nisin-treated products is that a given contaminated package would be considered not contaminated if the concentration of *Lm* in the package were to fall to less than one cell per package, resulting in a reduced prevalence of *Lm* contamination. A stochastic process of complete elimination was observed for *Lm* inoculated at 10^2 CFU/g on cold-smoked salmon that was then treated with 250 ppm of nisin *(14)*; thus, future models may benefit from refining the approach used to predict nisin-dependent elimination of *Lm* from a packaged product because the current approach may overestimate the prevalence reduction induced by nisin treatments.

Compared with nisin treatments, interventions that targeted a 50% reduction in the prevalence of *Lm* were less effective for reducing RR risks. However, the reduction in

RR risks achieved by a 50% reduction in *Lm* prevalence was considerably higher than reductions in RR risks that could be achieved by bacteriostatic growth inhibitors (potassium lactate and sodium diacetate) or by controlling storage temperature (which also reduced *Lm* growth and hence could be considered bacteriostatic). In contrast, reports of public health risk assessments for *Lm* have typically suggested that interventions that reduced growth (e.g., controlling storage and distribution temperatures and use of growth inhibitors) had a larger impact on frequency of human listeriosis cases than did interventions that reduced *Lm* prevalence *(28, 37, 66, 83)*. This difference in the effects of various control strategies on RR risks versus public health risks is logical and consistent with our knowledge of the biology of *Lm*. Most listeriosis cases are attributed to products contaminated with high levels of *Lm (65, 82)*. Based on current U.S. regulations, products positive for *Lm* in a 25-g sample will trigger a recall or other regulatory consequences regardless of the contamination level. Assuming reliable and sensitive tests, regulatory consequences are equally likely to be triggered by products that are contaminated at 100 and at 10 million *Lm* cells per package. Hence our model further illustrates the importance of regulatory policies based on the public health risk because policies based on only presence or absence of a hazard (e.g., *Lm*) may inadvertently incentivize interventions that prioritize reductions of RR risks over reductions of public health risks. Until new regulatory policies are implemented, processors face a dilemma as they decide on the relative importance of reducing RR risks and reducing public health risks associated with their products. Most likely, processor will try to comanage both types of risks, which means that some resources that will be dedicated to reducing RR risks would be better used to further reduce public health risks.

In conclusion, we developed a framework for a modeling approach for assessing the risk of food recalls or other regulatory consequences due to *Lm* contamination. Using this framework, the 3R model was developed as a decision support tool for producers to reduce the RR risks of cold-smoked salmon products through improvement of relevant data collection and/or identification and optimization of interventions for controlling *Lm*. The 3R model is complementary to but distinct from the existing public health risk assessment models because it focuses on assessing the risk of food recalls or other regulatory consequences instead of human listeriosis cases and thus bypasses the uncertainties associated with the dose-response compartment. The data gathered in this study indicate that reducing the prevalence of *Lm* contamination is more effective for reducing RR risks than is preventing the growth of *Lm* to high levels on contaminated products, which is more effective for reducing human listeriosis risks. This finding suggests a new paradigm for incorporating public health risk policies into the regulations for *Lm* in smoked seafood products because the current policies may inadvertently incentivize use of strategies that reduce RR risks over strategies that reduce public health risks (i.e., the risk of human listeriosis cases). Nisin treatment of cold-smoked salmon products was predicted to lead to the greatest reduction in RR risks, likely because of the dual effect of nisin for reducing both *Lm* prevalence and initial *Lm* contamination levels. To further improve the prediction of RR risks, resources should be focused on collection of data about *Lm* prevalence and initial contamination levels and product storage temperatures. Data for die-off and growth kinetic parameters of *Lm* on cold-smoked salmon treated with various antimicrobials can be used to expand the model to assess the impact of other antimicrobials on RR risks.

ACKNOWLEDGMENTS

This article is a product of project R/SHH-18 funded under award NA18OAR4170096 from the National Sea Grant College Program of the U.S. Department of Commerce, National Oceanic and Atmospheric Administration to the Research Foundation for the State University of New York Sea Grant. The statements, findings, conclusions, views, and recommendations are those of the author(s) and do not necessarily reflect the views of any of those organizations. We thank Dr. Renata Ivanek (Department of Population Medicine and Diagnostic Sciences, Cornell University) for suggestions about the statistical analysis.

SUPPLEMENTAL MATERIAL

Supplemental material associated with this article can be found online at: https://doi.org/10.4315/JFP-22-025.s1

REFERENCES

1. Afchain, A. L., E. Derens, J. Guilpart, and M. Cornu. 2005. Statistical modelling of cold-smoked salmon temperature profiles for risk assessment of *Listeria monocytogenes*. *Acta Hortic*. 674:383–388.
2. Akingbade, D., N. Bauer, S. Dennis, D. Gallagher, K. Hoelzer, J. Kause, R. Pouillot, M. Silverman, and J. Tang. 2013. Interagency retail *Listeria monocytogenes* risk assessment workgroup. Available at: https://www.fsis.usda.gov/sites/default/files/media_file/2020-07/Lm-Retail-Technical-Report.pdf. Accessed 7 June 2021.
3. Anderson, D. R. 2008. Model based inference in the life sciences: a primer on evidence. Springer-Verlag, New York.
4. Baranyi, J., and T. A. Roberts. 1994. A dynamic approach to predicting bacterial growth in food. *Int. J. Food Microbiol*. 23:277–294.
5. Beaufort, A., S. Rudelle, N. Gnanou-Besse, M. T. Toquin, A. Kerouanton, H. Bergis, G. Salvat, and M. Cornu. 2007. Prevalence and growth of *Listeria monocytogenes* in naturally contaminated cold-smoked salmon. *Lett. Appl. Microbiol*. 44:406–411.
6. Buchanan, R. L., L. G. M. Gorris, M. M. Hayman, T. C. Jackson, and R. C. Whiting. 2017. A review of *Listeria monocytogenes*: an update on outbreaks, virulence, dose-response, ecology, and risk assessments. *Food Control* 75:1–13.
7. Buchanan, R. L., R. C. Whiting, and W. C. Damert. 1997. When is simple good enough: a comparison of the Gompertz, Baranyi, and three-phase linear models for fitting bacterial growth curves. *Food Microbiol*. 14:313–326.
8. Buehler, A. J., N. H. Martin, K. J. Boor, and M. Wiedmann. 2018. Psychrotolerant spore-former growth characterization for the development of a dairy spoilage predictive model. *J. Dairy Sci*. 101:6964–6981.
9. Burnham, K. P., and D. R. Anderson. 2002. Model selection and multimodel inference: a practical information-theoretic approach, 2nd ed. Springer-Verlag, New York.
10. Carnell, R. 2020. lhs: Latin hypercube samples. R package version 1.1.1. Available at: https://CRAN.R-project.org/package=lhs. Accessed 1 February 2022.
11. Centers for Disease Control and Prevention. 2021. *Listeria* (listeriosis). CDC. Available at: https://www.cdc.gov/listeria/index.html. Accessed 7 June 2021.
12. Centers for Disease Control and Prevention. 2021. National Outbreak Reporting System (NORS) dashboard. CDC. Available at: https://wwwn.cdc.gov/norsdashboard/. Accessed 1 July 2020.

13. Chen, R., J. Skeens, R. H. Orsi, M. Wiedmann, and V. Guariglia-Oropeza. 2020. Pre-growth conditions and strain diversity affect nisin treatment efficacy against *Listeria monocytogenes* on cold-smoked salmon. *Int. J. Food Microbiol*. 333:108793.
14. Chen, R., J. Skeens, M. Wiedmann, and V. Guariglia-Oropeza. Unpublished data.
15. Codex Alimentarius Commission. 2003. Principles and guidelines for the conduct of microbiological risk assessment. CAC/GL-30. Available at: http://www.fao.org/3/y1579e/y1579e05.htm. Accessed 8 June 2021.
16. Cohen, J. 1988. Statistical power analysis for the behavioral sciences, 2nd ed. Erlbaum, Hillsdale, NJ.
17. Cohen, J. 1992. A power primer. *Psychol*. *Bull*. 112:155–159.
18. Cornu, M., A. Beaufort, S. Rudelle, L. Laloux, H. Bergis, N. Miconnet, T. Serot, and M. L. Delignette-Muller. 2006. Effect of temperature, water-phase salt and phenolic contents on *Listeria monocytogenes* growth rates on cold-smoked salmon and evaluation of secondary models. *Int. J. Food Microbiol*. 106:159–168.
19. Dalgaard, P., and L. Vigel Jørgensen. 1998. Predicted and observed growth of *Listeria monocytogenes* in seafood challenge tests and in naturally contaminated cold-smoked salmon. *Int. J. Food Microbiol*. 40:105–115.
20. Delignette-Muller, M. L., M. Cornu, R. Pouillot, and J.-B. Denis. 2006. Use of Bayesian modelling in risk assessment: application to growth of *Listeria monocytogenes* and food flora in cold-smoked salmon. *Int. J. Food Microbiol*. 106:195–208.
21. Delignette-Muller, M. L., and C. Dutang. 2015. fitdistrplus: an R package for fitting distributions. *J. Stat. Soft*. 64:1–34.
22. Ding, T., J. Iwahori, F. Kasuga, J. Wang, F. Forghani, M.-S. Park, and D.-H. Oh. 2013. Risk assessment for *Listeria monocytogenes* on lettuce from farm to table in Korea. *Food Control* 30:190–199.
23. Duffes, F., C. Corre, F. Leroi, X. Dousset, and P. Boyaval. 1999. Inhibition of *Listeria monocytogenes* by in situ produced and semipurified bacteriocins of *Carnobacterium* spp. on vacuum-packed, refrigerated cold-smoked salmon. *J. Food Prot*. 62:1394–1403.
24. Elzhov, T., K. Mullen, A.-N. Spiess, and B. Bolker. 2016. minpack.lm: R interface to the Levenberg-Marquardt nonlinear least-squares algorithm found in MINPACK, plus support for bounds. R package version 1.2-1. Available at: https://CRAN.R-project.org/package=minpack.lm. Accessed 1 February 2022.
25. Evans, M. R., B. Swaminathan, L. M. Graves, E. Altermann, T. R. Klaenhammer, R. C. Fink, S. Kernodle, and S. Kathariou. 2004. Genetic markers unique to *Listeria monocytogenes* serotype 4b differentiate epidemic clone II (hot dog outbreak strains) from other lineages. *Appl. Environ. Microbiol*. 70:2383–2390.
26. Ferreira, V., M. Wiedmann, P. Teixeira, and M. J. Stasiewicz. 2014. *Listeria monocytogenes* persistence in food-associated environments: epidemiology, strain characteristics, and implications for public health. *J. Food Prot*. 77:150–170.
27. Frey, H. C. 1992. Quantitative analysis of uncertainty and variability in environmental policy making. Fellowship Program for Environmental Science and Engineering, American Association for the Advancement of Science, Washington, DC.
28. Gallagher, D., R. Pouillot, K. Hoelzer, J. Tang, S. B. Dennis, and J. R. Kause. 2016. *Listeria monocytogenes* in retail delicatessens: an interagency risk assessment—risk mitigations. *J. Food Prot*. 79:1076–1088.
29. Gaul, L. K., N. H. Farag, T. Shim, M. A. Kingsley, B. J. Silk, and E. Hyytia-Trees. 2013. Hospital-acquired listeriosis outbreak caused by contaminated diced celery—Texas, 2010. *Clin. Infect. Dis*. 56:20–26.
30. Gibson, A. M., N. Bratchell, and T. A. Roberts. 1988. Predicting microbial growth: growth responses of salmonellae in a laboratory medium as affected by pH, sodium chloride and storage temperature. *Int. J. Food Microbiol*. 6:155–178.
31. Gombas, D. E., Y. Chen, R. S. Clavero, and V. N. Scott. 2003. Survey of *Listeria monocytogenes* in ready-to-eat foods. *J. Food Prot*. 66:559–569.
32. Goulet, V., and P. Marchetti. 1996. Listeriosis in 225 non-pregnant patients in 1992: clinical aspects and outcome in relation to predisposing conditions. *Scand*. *J. Infect. Dis*. 28:367–374.
33. Guenther, S., D. Huwyler, S. Richard, and M. J. Loessner. 2009. Virulent bacteriophage for efficient biocontrol of *Listeria monocytogenes* in ready-to-eat foods. *Appl. Environ. Microbiol*. 75:93–100.
34. Hartig, F., F. Minunno, and S. Paul. 2019. BayesianTools: general-purpose MCMC and SMC samplers and tools for Bayesian statistics. R package version 0.1.7. Available at: https://CRAN.R-project.org/package=BayesianTools. Accessed 1 February 2022.
35. Hudson, J. A., C. Billington, G. Carey-Smith, and G. Greening. 2005. Bacteriophages as biocontrol agents in food. *J. Food Prot*. 68:426–437.
36. Hudson, J. A., and S. J. Mott. 1993. Growth of *Listeria monocytogenes, Aeromonas hydrophila* and *Yersinia enterocolitica* on cold-smoked salmon under refrigeration and mild temperature abuse. *Food Microbiol*. 10:61–68.
37. ILSI Research Foundation, Risk Science Institute, Expert Panel on *Listeria monocytogenes* in Foods. 2005. Achieving continuous improvement in reductions in foodborne listeriosis—a risk-based approach. *J. Food Prot*. 68:1932–1994.
38. Jami, M., M. Ghanbari, M. Zunabovic, K. J. Domig, and W. Kneifel. 2014. *Listeria monocytogenes* in aquatic food products—a review. *Compr. Rev. Food Sci. Food Saf*. 13:798–813.
39. Jensen, A., W. Frederiksen, and P. Gerner-Smidt. 1994. Risk factors for listeriosis in Denmark, 1989–1990. *Scand*. *J. Infect. Dis*. 26:171–178.
40. Kang, J., M. J. Stasiewicz, K. J. Boor, M. Wiedmann, and T. M. Bergholz. 2014. Optimization of combinations of bactericidal and bacteriostatic treatments to control *Listeria monocytogenes* on cold-smoked salmon. *Int. J. Food Microbiol*. 179:1–9.
41. Kendall, M. G., and A. Stuart. 1979. The advanced theory of statistics, 4th ed. Macmillan, New York.
42. Lappi, V. R., A. Ho, K. Gall, and M. Wiedmann. 2004. Prevalence and growth of *Listeria* on naturally contaminated smoked salmon over 28 days of storage at 4°C. *J. Food Prot*. 67:1022–1026.
43. Lindqvist, R., and A. Westöö. 2000. Quantitative risk assessment for *Listeria monocytogenes* in smoked or gravad salmon and rainbow trout in Sweden. *Int. J. Food Microbiol*. 58:181–196.
44. Link, W. A., and R. J. Barker. 2006. Model weights and the foundations of multimodel inference. *Ecology* 87:2626–2635.
45. Mafart, P., O. Couvert, S. Gaillard, and I. Leguerinel. 2002. On calculating sterility in thermal preservation methods: application of the Weibull frequency distribution model. *Int. J. Food Microbiol*. 72:107–113.
46. Marino, S., I. B. Hogue, C. J. Ray, and D. E. Kirschner. 2008. A methodology for performing global uncertainty and sensitivity analysis in systems biology. *J. Theor. Biol*. 254:178–196.
47. Mazerolle, M. J. 2020. AICcmodavg: model selection and multimodel inference based on (Q)AIC(c). R package version 2.3-1. Available at: https://cran.r-project.org/package=AICcmodavg. Accessed 1 February 2022.
48. Mejlholm, O., N. Bøknæs, and P. Dalgaard. 2015. Development and validation of a stochastic model for potential growth of *Listeria monocytogenes* in naturally contaminated lightly preserved seafood. *Food Microbiol*. 45:276–289.
49. Mejlholm, O., and P. Dalgaard. 2007. Modeling and predicting the growth of lactic acid bacteria in lightly preserved seafood and their inhibiting effect on *Listeria monocytogenes*. *J. Food Prot*. 70:70–84.
50. Mejlholm, O., and P. Dalgaard. 2009. Development and validation of an extensive growth and growth boundary model for *Listeria monocytogenes* in lightly preserved and ready-to-eat shrimp. *J. Food Prot*. 72:2132–2143.
51. Mejlholm, O., and P. Dalgaard. 2015. Modelling and predicting the simultaneous growth of *Listeria monocytogenes* and psychrotolerant lactic acid bacteria in processed seafood and mayonnaise-based seafood salads. *Food Microbiol*. 46:1–14.
52. Miconnet, N., M. Cornu, A. Beaufort, L. Rosso, and J.-B. Denis. 2005. Uncertainty distribution associated with estimating a proportion in microbial risk assessment. *Risk Anal*. 25:39–48.
53. Mokhtari, A., and H. C. Frey. 2005. Sensitivity analysis of a two-dimensional probabilistic risk assessment model using analysis of variance. *Risk Anal*. 25:1511–1529.
54. Montiel, R., D. Bravo, M. de Alba, P. Gaya, and M. Medina. 2012. Combined effect of high pressure treatments and the lactoperoxidase

system on the inactivation of *Listeria monocytogenes* in cold-smoked salmon. *Innov. Food Sci. Emerg. Technol*. 16:26–32.
55. National Research Council. 1994. Science and judgment in risk assessment. National Academies Press, Washington, DC.
56. Nauta, M. J. 2000. Separation of uncertainty and variability in quantitative microbial risk assessment models. *Int. J. Food Microbiol*. 57:9–18.
57. Neetoo, H., M. Ye, H. Chen, R. D. Joerger, D. T. Hicks, and D. G. Hoover. 2008. Use of nisin-coated plastic films to control *Listeria monocytogenes* on vacuum-packaged cold-smoked salmon. *Int. J. Food Microbiol*. 122:8–15.
58. Nightingale, K. K., Y. H. Schukken, C. R. Nightingale, E. D. Fortes, A. J. Ho, Z. Her, Y. T. Grohn, P. L. McDonough, and M. Wiedmann. 2004. Ecology and transmission of *Listeria monocytogenes* infecting ruminants and in the farm environment. *Appl. Environ. Microbiol*. 70:4458–4467.
59. Nilsson, L., L. Gram, and H. H. Huss. 1999. Growth control of *Listeria monocytogenes* on cold-smoked salmon using a competitive lactic acid bacteria flora. *J. Food Prot*. 62:336–342.
60. Nilsson, L., H. Henrik Huss, and L. Gram. 1997. Inhibition of *Listeria monocytogenes* on cold-smoked salmon by nisin and carbon dioxide atmosphere. *Int. J. Food Microbiol*. 38:217–227.
61. Olsen, S. J., M. Patrick, S. B. Hunter, V. Reddy, L. Kornstein, W. R. MacKenzie, K. Lane, S. Bidol, G. A. Stoltman, D. M. Frye, I. Lee, S. Hurd, T. F. Jones, T. N. LaPorte, W. Dewitt, L. Graves, M. Wiedmann, D. J. Schoonmaker-Bopp, A. J. Huang, C. Vincent, A. Bugenhagen, J. Corby, E. R. Carloni, M. E. Holcomb, R. F. Woron, S. M. Zansky, G. Dowdle, F. Smith, S. Ahrabi-Fard, A. R. Ong, N. Tucker, N. A. Hynes, and P. Mead. 2005. Multistate outbreak of *Listeria monocytogenes* infection linked to delicatessen turkey meat. *Clin. Infect. Dis*. 40:962–967.
62. Pelroy, G., M. Peterson, R. Paranjpye, J. Almond, and M. Eklund. 1994. Inhibition of *Listeria monocytogenes* in cold-process (smoked) salmon by sodium nitrite and packaging method. *J. Food Prot*. 57:114–119.
63. Pelroy, G. A., M. E. Peterson, P. J. Holland, and M. W. Eklund. 1994. Inhibition of *Listeria monocytogenes* in cold-process (smoked) salmon by sodium lactate. *J. Food Prot*. 57:108–113.
64. Pouillot, R., P. Beaudeau, J. Denis, F. Derouin, and AFSSA *Cryptosporidium* Study Group. 2004. A quantitative risk assessment of waterborne cryptosporidiosis in France using second-order Monte Carlo simulation. *Risk Anal*. 24:1–17.
65. Pouillot, R., V. Goulet, M. L. Delignette-Muller, A. Mahé, and M. Cornu. 2009. Quantitative risk assessment of *Listeria monocytogenes* in French cold-smoked salmon. II. Risk characterization. *Risk Anal*. 29:806–819.
66. Pouillot, R., N. Miconnet, A.-L. Afchain, M. L. Delignette-Muller, A. Beaufort, L. Rosso, J.-B. Denis, and M. Cornu. 2007. Quantitative risk assessment of *Listeria monocytogenes* in French cold-smoked salmon. I. Quantitative exposure assessment. *Risk Anal*. 27:683–700.
67. Pradhan, A. K., R. Ivanek, Y. T. Gröhn, R. Bukowski, I. Geornaras, J. N. Sofos, and M. Wiedmann. 2010. Quantitative risk assessment of listeriosis-associated deaths due to *Listeria monocytogenes* contamination of deli meats originating from manufacture and retail. *J. Food Prot*. 73:620–630.
68. Pradhan, A. K., R. Ivanek, Y. T. Gröhn, I. Geornaras, J. N. Sofos, and M. Wiedmann. 2009. Quantitative risk assessment for *Listeria monocytogenes* in selected categories of deli meats: impact of lactate and diacetate on listeriosis cases and deaths. *J. Food Prot*. 72:978–989.
69. Ratkowsky, D. A., J. Olley, T. A. McMeekin, and A. Ball. 1982. Relationship between temperature and growth rate of bacterial cultures. *J. Bacteriol*. 149:1–5.
70. R Core Team. 2021. R: a language and environment for statistical computing. R Foundation for Statistical Computing, Vienna.
71. Ricci, A., A. Allende, D. Bolton, M. Chemaly, R. Davies, P. S. F. Escámez, R. Girones, L. Herman, K. Koutsoumanis, B. Nørrung, L. Robertson, G. Ru, M. Sanaa, M. Simmons, P. Skandamis, E. Snary, N. Speybroeck, B. T. Kuile, J. Threlfall, H. Wahlström, J. Takkinen, M. Wagner, D. Arcella, M. T. D. S. Felicio, M. Georgiadis, W. Messens, and R. Lindqvist. 2018. *Listeria monocytogenes* contamination of ready-to-eat foods and the risk for human health in the EU. *EFSA J*. 16:e05134.
72. Scallan, E., R. M. Hoekstra, F. J. Angulo, R. V. Tauxe, M.-A. Widdowson, S. L. Roy, J. L. Jones, and P. M. Griffin. 2011. Foodborne illness acquired in the United States—major pathogens. *Emerg. Infect. Dis*. 17:7–15.
73. Stephens, M. A. 1986. Tests based on EDF statistics, p. 97–194. *In* R. D'Agostino (ed.), Goodness-of-fit techniques. Routledge, Abingdon, UK.
74. Stevenson, M., E. Sergeant, T. Nunes, C. Heuer, and J. Marshall. 2021. epiR: tools for the analysis of epidemiological data. R package version 2.0.19. Available at: https://CRAN.R-project.org/package=epiR. Accessed 1 February 2022.
75. Szabo, E. A., and M. E. Cahill. 1999. Nisin and ALTATM 2341 inhibit the growth of *Listeria monocytogenes* on smoked salmon packaged under vacuum or 100% CO_2. *Lett. Appl. Microbiol*. 28:373–377.
76. Tang, S., M. J. Stasiewicz, M. Wiedmann, K. J. Boor, and T. M. Bergholz. 2013. Efficacy of different antimicrobials on inhibition of *Listeria monocytogenes* growth in laboratory medium and on cold-smoked salmon. *Int. J. Food Microbiol*. 165:265–275.
77. Thimothe, J., K. K. Nightingale, K. Gall, V. N. Scott, and M. Wiedmann. 2004. Tracking of *Listeria monocytogenes* in smoked fish processing plants. *J. Food Prot*. 67:328–341.
78. Tompkin, R. B. 2002. Control of *Listeria monocytogenes* in the food-processing environment. *J. Food Prot*. 65:709–725.
79. U.S. Food and Drug Administration. 2021. Food Code 2013. Available at: https://www.fda.gov/media/87140/download. Accessed 7 June 2021.
80. U.S. Food and Drug Administration. 2021. Recalls, market withdrawals, & safety alerts. Available at: https://www.fda.gov/safety/recalls-market-withdrawals-safety-alerts. Accessed 7 June 2021.
81. U.S. Food and Drug Administration, Center for Food Safety and Applied Nutrition. 2017. Detection of *Listeria monocytogenes* in foods and environmental samples, and enumeration of *Listeria monocytogenes* in foods, chap. 10. *In* Bacteriological analytical manual. Available at: https://www.fda.gov/media/90488/download. Accessed 7 June 2021.
82. U.S. Food and Drug Administration, Center for Food Safety and Applied Nutrition and U.S. Department of Agriculture, Food Safety and Inspection Service. 2003. Quantitative assessment of relative risk to public health from foodborne *Listeria monocytogenes* among selected categories of ready-to-eat foods. Available at: https://www.fda.gov/media/124721/download. Accessed 30 June 2021.
83. U.S. Food and Drug Administration and Health Canada. 2015. Joint FDA/Health Canada quantitative assessment of the risk of listeriosis from soft-ripened cheese consumption in the United States and Canada. Available at: https://www.fda.gov/safety/recalls-market-withdrawals-safety-alerts. Accessed 7 June 2021.
84. Vásquez, G. A., P. Busschaert, L. U. Haberbeck, M. Uyttendaele, and A. H. Geeraerd. 2014. An educationally inspired illustration of two-dimensional quantitative microbiological risk assessment (QMRA) and sensitivity analysis. *Int. J. Food Microbiol*. 190:31–43.
85. Vose, D. 2008. Risk analysis: a quantitative guide, 3rd ed. Wiley, Chichester, UK.
86. Ye, M., H. Neetoo, and H. Chen. 2008. Effectiveness of chitosan-coated plastic films incorporating antimicrobials in inhibition of *Listeria monocytogenes* on cold-smoked salmon. *Int. J. Food Microbiol*. 127:235–240.
87. Zhu, M. J., A. Mendonca, H. A. Ismail, M. Du, E. J. Lee, and D. U. Ahn. 2005. Impact of antimicrobial ingredients and irradiation on the survival of *Listeria monocytogenes* and the quality of ready-to-eat turkey ham. *Poult. Sci*. 84:613–620.
88. Zoellner, C., M. Wiedmann, and R. Ivanek. 2019. An assessment of listeriosis risk associated with a contaminated production lot of frozen vegetables consumed under alternative consumer handling scenarios. *J. Food Prot*. 82:2174–2193.
89. Zwietering, M. H., I. Jongenburger, F. M. Rombouts, and K. van 't Riet. 1990. Modeling of the bacterial growth curve. *Appl. Environ. Microbiol*. 56:1875–1881.